



Measurement of the production cross-section of J/ψ and $\psi(2S)$ mesons in pp collisions at $\sqrt{s} = 13$ TeV with the ATLAS detector

ATLAS Collaboration*

CERN, 1211 Geneva 23, Switzerland

Received: 4 October 2023 / Accepted: 12 January 2024 / Published online: 19 February 2024
© CERN for the benefit of The ATLAS Collaboration 2024

Abstract Measurements of the differential production cross-sections of prompt and non-prompt J/ψ and $\psi(2S)$ mesons with transverse momenta between 8 and 360 GeV and rapidity in the range $|y| < 2$ are reported. Furthermore, measurements of the non-prompt fractions of J/ψ and $\psi(2S)$, and the prompt and non-prompt $\psi(2S)$ -to- J/ψ production ratios, are presented. The analysis is performed using 140 fb^{-1} of $\sqrt{s} = 13$ TeV pp collision data recorded by the ATLAS detector at the LHC during the years 2015–2018.

1 Introduction

Studies involving heavy quarkonia provide a unique insight into the nature of quantum chromodynamics (QCD) near the boundary of the perturbative and non-perturbative regimes. However, despite a long history of research, quarkonium production in hadronic collisions still presents significant challenges to both theory and experiment.

In high-energy hadronic collisions, charmonium states can be produced either from short-lived QCD sources (referred to as *prompt* production) or from long-lived sources – decays of beauty hadrons (*non-prompt* production). These two sources can be distinguished experimentally by measuring the distance between the production and decay vertices of the charmonium state. Feed-down decays of higher charmonium states contribute to the production of J/ψ mesons for both of these sources, and should be taken into account when comparing with theoretical predictions (there is no significant feed-down contribution to $\psi(2S)$ production). While calculations within the framework of perturbative QCD (see e.g. Refs. [1, 2]) have been reasonably successful in describing the non-prompt contributions, a satisfactory understanding of the prompt production mechanisms is still to be achieved.

Methods developed within the non-relativistic QCD (NRQCD) approach provide a framework for describing quarkonium production processes, leading to a variety of models differing in their accuracy and predictive power. In par-

ticular, Ref. [3] introduced a number of phenomenological parameters – long-distance matrix elements (LDMEs) – which can be extracted from fits to the experimental data, and are expected to describe the cross-sections and differential spectra for several sets of data reasonably well [4–7]. However, various attempts to build a universal library of LDMEs to be used to describe a wider range of measurements such as the polarisation of quarkonia [8–11], their associated production [12, 13] or the production of quarkonium in a wider range of processes (e.g. photo- and electro-production) have not been particularly successful [14–18]. An alternative approach to the description of the hadronisation process of heavy quarkonia is offered by the Colour Evaporation Model (CEM) [19–21], which offers a simpler framework with fewer parameters, but has its own problems in describing the data [22]. A combination of ATLAS results with cross-section and polarisation measurements from CMS [7, 23, 24], LHCb [6, 25–29] and ALICE [11, 30–36] now includes a variety of charmonium production characteristics in a wide kinematic range, thus providing a wealth of information for a new generation of theoretical models.

One way to add qualitatively new information is to extend the kinematic range of quarkonium production measurements. ATLAS has previously measured the inclusive differential cross-section for J/ψ production in pp collisions at $\sqrt{s} = 7$ and 8 TeV [4], as well as the differential cross-sections for the production of χ_c states [37], and for $\psi(2S)$ production [5]. In most of these measurements, ATLAS exploited a dimuon trigger with a muon transverse momentum (p_T) threshold of 4 GeV, with the high- p_T reach limited mainly by the dimuon trigger's performance to about 100 GeV: at higher p_T values the angular resolution of the muon trigger system is not sufficient to separate the two almost collinear muons. This paper describes a measurement of J/ψ ($\psi(2S)$) meson production via decay in the dimuon channel, at $\sqrt{s} = 13$ TeV for meson transverse momenta of 8–360 GeV (8–140 GeV), which is a much broader range than in previous measurements. This was made possible by the use of two different triggers. Production of J/ψ and

* e-mail: atlas.publications@cern.ch

$\psi(2S)$ at low p_T , between 8 and 60 GeV, is measured using a dimuon trigger requiring a pair of muons to each pass a p_T threshold of 4 GeV, while at high p_T a single-muon trigger with a p_T threshold of 50 GeV was used. This allowed measurements to be performed for transverse momenta as high as 360 GeV for J/ψ and 140 GeV for $\psi(2S)$. The measurements include the double-differential cross-sections for production of the two vector charmonium states (separately for the prompt and non-prompt production mechanisms), the non-prompt fraction for each state, and the prompt and non-prompt $\psi(2S)$ -to- J/ψ production ratios.

The paper is organised as follows. A brief description of the ATLAS detector is given in Sect. 2. The event selection and the analysis strategy are explained in Sect. 3, followed by a description of the systematic uncertainties affecting the measurement in Sect. 4. Results and comparisons with theoretical calculations are presented in Sect. 5, followed by a summary in Sect. 6.

2 The ATLAS detector

The ATLAS experiment [38] at the LHC is a multipurpose particle detector with a forward–backward symmetric cylindrical geometry and a near 4π coverage in solid angle.¹ It consists of an inner tracking detector (ID) surrounded by a thin superconducting solenoid providing a 2 T axial magnetic field, electromagnetic and hadron calorimeters, and a muon spectrometer. The inner tracking detector covers the pseudorapidity range $|\eta| < 2.5$. It consists of silicon pixel, silicon microstrip, and transition radiation tracking detectors. Metal/liquid-argon (LAr) sampling calorimeters provide electromagnetic (EM) energy measurements with high granularity. A steel/scintillator-tile hadron calorimeter covers the central pseudorapidity range ($|\eta| < 1.7$). The endcap and forward regions are instrumented with LAr calorimeters for both the EM and hadronic energy measurements up to $|\eta| = 4.9$. The muon spectrometer surrounds the calorimeters and is based on three large superconducting air-core toroidal magnets with eight coils each. The field integral of the toroids ranges between 2.0 and 6.0 T m across most of the detector. The muon spectrometer has a system of precision chambers for tracking and fast detectors for triggering. A two-level trigger system is used to select events. The first-level trigger is implemented in hardware and uses a subset

¹ ATLAS uses a right-handed coordinate system with its origin at the nominal interaction point (IP) in the centre of the detector and the z -axis along the beam pipe. The x -axis points from the IP to the centre of the LHC ring, and the y -axis points upwards. Cylindrical coordinates (r, ϕ) are used in the transverse plane, ϕ being the azimuthal angle around the z -axis. The pseudorapidity is defined in terms of the polar angle θ as $\eta = -\ln \tan(\theta/2)$. Angular distance is measured in units of $\Delta R \equiv \sqrt{(\Delta\eta)^2 + (\Delta\phi)^2}$.

of the detector information to accept events at a rate below 100 kHz. This is followed by a software-based trigger that reduces the accepted event rate to 1 kHz on average depending on the data-taking conditions. An extensive software suite [39] is used in data simulation, in the reconstruction and analysis of real and simulated data, in detector operations, and in the trigger and data acquisition systems of the experiment.

3 Analysis strategy

3.1 Event selection

Data for this analysis were taken during the LHC proton–proton collision runs at $\sqrt{s} = 13$ TeV in the years 2015–2018. For lower values of the transverse momentum p_T of the dimuon system, between 8 and 60 GeV, a dimuon trigger was used, requiring a pair of muons to each pass a p_T threshold of 4 GeV. This trigger ran unprescaled during 2015 data-taking, collecting an integrated luminosity of 2.6 fb^{-1} . In the high p_T range between 60 and 360 GeV, a single-muon trigger with a p_T threshold of 50 GeV was used, unprescaled throughout the full Run 2 data-taking, providing a total integrated luminosity of 140 fb^{-1} . The selected events were required to contain a pair of oppositely charged muons of high quality (using the *tight* identification requirements defined in Ref. [40]), with $p_T > 4$ GeV and $|\eta| < 2.4$. In the low p_T range the two muons were required to match the two trigger objects of the dimuon trigger, while in the high p_T range at least one of the muons was required to have $p_T > 52.5$ GeV and match the trigger object. The two ID tracks attributed to the muons were fitted to a common vertex, and the dimuon invariant mass $m_{\mu\mu}$ was required to satisfy $2.6 < m_{\mu\mu} < 4.2$ GeV. The transverse distance L_{xy} between the primary vertex and the dimuon vertex was used to calculate the meson’s pseudo-proper decay time

$$\tau = \frac{m_{\mu\mu}}{p_T} \frac{L_{xy}}{c},$$

where p_T is the reconstructed transverse momentum of the dimuon system, and c is the speed of light. The primary vertex is chosen as the reconstructed collision interaction vertex whose z coordinate is nearest to the point of closest approach of the dimuon system’s trajectory to the beam axis. If an event has more than one selected dimuon candidate, all candidates are retained and treated independently.

3.2 Cross-section determination

The phase space of the measurement is divided into 34 intervals in dimuon p_T covering the range from 8 to 360 GeV,

Table 1 Parameterisation of the fit model. Here G , CB , E and P denote Gaussian, Crystal Ball, exponential and second-order polynomial functions, respectively, with different indices corresponding to different

parameters. The parameterisation of the $i = 1$ term is modified as described in the text and shown in Eq. (4)

i	Type	P/NP	$f_i(m)$	$h_i(\tau)$
1	J/ψ	P	$\omega_0 G_1(m) + (1 - \omega_0)[\omega_1 CB(m) + (1 - \omega_1)G_2(m)]$	$\delta(\tau)$
2	J/ψ	NP	$\omega_0 G_1(m) + (1 - \omega_0)[\omega_1 CB(m) + (1 - \omega_1)G_2(m)]$	$\omega_2 E_1(\tau) + (1 - \omega_2)E_1(b\tau)$
3	$\psi(2S)$	P	$\omega_0 G_1(\beta m) + (1 - \omega_0)[\omega_1 CB(\beta m) + (1 - \omega_1)G_2(\beta m)]$	$\delta(\tau)$
4	$\psi(2S)$	NP	$\omega_0 G_1(\beta m) + (1 - \omega_0)[\omega_1 CB(\beta m) + (1 - \omega_1)G_2(\beta m)]$	$E_2(\tau)$
5	Bkg	P	P	$\delta(\tau)$
6	Bkg	NP	$E_3(m)$	$E_4(\tau)$
7	Bkg	NP	$E_5(m)$	$E_6(\tau)$

and 3 intervals in absolute rapidity² $|y|$ with boundaries at 0, 0.75, 1.5 and 2.0, thus producing 102 analysis bins overall. In each (p_T, y) bin, a two-dimensional unbinned maximum-likelihood fit to the distribution of dimuon candidates in invariant mass $m_{\mu\mu}$ and pseudo-proper decay time τ of the ψ meson is performed to obtain the raw yields $N_{\psi}^{P, NP}$ for prompt (P) and non-prompt (NP) ψ mesons, where $\psi = J/\psi, \psi(2S)$. The raw yields are then corrected to account for the geometrical acceptance $\mathcal{A}(\psi)$, the trigger and reconstruction efficiencies ϵ_{trig} and ϵ_{reco} , and the trigger and reconstruction correction scale factors ϵ_{trigSF} and ϵ_{recoSF} , averaged over that bin. Several low p_T bins are divided into narrower sub-bins to obtain raw yields in finer granularity, which are then corrected and summed to give the final yield in the corresponding analysis bin. This procedure helps to reduce measurement biases due to modelling assumptions in the regions of phase space with large statistical power.

The prompt (P) and non-prompt (NP) double-differential production cross-sections for $\psi = J/\psi, \psi(2S)$ in each analysis bin are calculated as

$$\frac{d^2\sigma^{P, NP}(pp \rightarrow \psi)}{dp_T dy} \times \mathcal{B}(\psi \rightarrow \mu^+ \mu^-) = \frac{1}{\mathcal{A}(\psi)\epsilon_{\text{trig}}\epsilon_{\text{trigSF}}\epsilon_{\text{reco}}\epsilon_{\text{recoSF}}} \frac{N_{\psi}^{P, NP}}{\Delta p_T \Delta y \int \mathcal{L} dt}, \quad (1)$$

where Δp_T and Δy are bin widths in p_T and rapidity, and $\int \mathcal{L} dt$ is the corresponding integrated luminosity. Bin migration effects are discussed in Sect. 3.4. The acceptance $\mathcal{A}(\psi)$ is defined as the probability that a ψ state with (true) momentum within an analysis bin survives the following acceptance selections imposed on the two muons (assuming $p_T(\mu_1) > p_T(\mu_2)$) in the two ψ p_T ranges:

- low p_T range, $p_T(\psi) < 60$ GeV: $p_T(\mu_1) > 4$ GeV, $p_T(\mu_2) > 4$ GeV, $|\eta(\mu_1)|, |\eta(\mu_2)| < 2.4$;

² Rapidity y of a particle of energy E and longitudinal momentum p_z is defined as $y = \frac{1}{2} \log \frac{E+p_z}{E-p_z}$.

- high p_T range, $p_T(\psi) \geq 60$ GeV: $p_T(\mu_1) > 52.5$ GeV, $p_T(\mu_2) > 4$ GeV, $|\eta(\mu_1)|, |\eta(\mu_2)| < 2.4$.

The acceptance calculation is performed using Monte Carlo (MC) generator-level kinematic variables, with resolution effects taken into account at the efficiency correction stage. An isotropic angular distribution of muons in the ψ decay frame is assumed. Since the spin alignment of the ψ states may affect the acceptance, a number of non-isotropic spin-alignment scenarios are used to calculate correction factors for the measured cross-sections (see Appendix). For a given spin-alignment scenario, systematic uncertainties due to the acceptance calculation are small (see Sect. 4). Changing to a different spin-alignment scenario, however, can lead to noticeable changes in the cross-sections and other measured quantities, including variations as a function of p_T (see Sect. 5).

The reconstruction efficiency ϵ_{reco} and trigger efficiency ϵ_{trig} are calculated using samples of fully simulated J/ψ and $\psi(2S)$ events, including appropriate trigger information. Correction scale factors ϵ_{recoSF} and ϵ_{trigSF} account for the differences between simulated and real data. See Sect. 3.4 for more details.

The non-prompt fractions for $\psi = J/\psi, \psi(2S)$ are defined as

$$F_{\psi}^{\text{NP}}(p_T, y) = \frac{d^2\sigma^{\text{NP}}(pp \rightarrow \psi)}{dp_T dy} \times \left[\frac{d^2\sigma^{\text{P}}(pp \rightarrow \psi)}{dp_T dy} + \frac{d^2\sigma^{\text{NP}}(pp \rightarrow \psi)}{dp_T dy} \right]^{-1}. \quad (2)$$

Finally, $\psi(2S)$ -to- J/ψ production ratios are defined separately for the prompt and non-prompt production mechanisms as

$$R^{P, NP}(p_T, y) = \frac{d^2\sigma^{P, NP}(pp \rightarrow \psi(2S))}{dp_T dy} \times \mathcal{B}(\psi(2S) \rightarrow \mu^+ \mu^-)$$

$$\times \left[\frac{d^2\sigma^{\text{P,NP}}(pp \rightarrow J/\psi)}{dp_T dy} \times \mathcal{B}(J/\psi \rightarrow \mu^+\mu^-) \right]^{-1}. \quad (3)$$

In calculating these quantities, the event yields, efficiencies, and acceptance corrections are used in accord with Eq. (1); uncertainties in the fraction and ratio measurements partially cancel out.

3.3 Fit model

The fit model's probability distribution function $F(m_{\mu\mu}, \tau)$ contains seven terms,

$$F(m_{\mu\mu}, \tau) = \sum_{i=1}^7 \kappa_i P_i(m_{\mu\mu}, \tau),$$

with fractions κ_i , describing four signal contributions and three types of background. Terms $i = 1, 2$ describe prompt and non-prompt J/ψ signal respectively; terms $i = 3, 4$ correspond to prompt and non-prompt $\psi(2S)$ signal. Term $i = 5$ describes the prompt background, where non-resonant dimuons are produced at the primary vertex (e.g. Drell–Yan pairs). Term $i = 6$ describes single-sided non-prompt background, mainly for dimuon continuum events where the two muons originate from the (cascade) decay of a single b -hadron, while term $i = 7$ describes the double-sided part of the non-prompt continuum, where the two muons originate from different b -hadrons, yielding a secondary vertex which may appear on either side of the beamline. For $i = 2-7$, each term is factorised into a function $f_i(m_{\mu\mu})$ of dimuon mass $m_{\mu\mu}$ and a function $h_i(\tau)$ of pseudo-proper decay time τ , where the latter is convolved with a decay time resolution function $R(\tau)$:

$$P_i(m_{\mu\mu}, \tau) = f_i(m_{\mu\mu}) \cdot [h_i(\tau) \otimes R(\tau)].$$

The term with $i = 1$, which describes the prompt J/ψ peak, has a similar structure but allows for some correlations between $m_{\mu\mu}$ and τ , as described below.

The decay time resolution function $R(\tau)$ is parameterised as a sum of three Gaussian functions, G_A , G_B and G_C , with the relative weights of the first two, ω_A and ω_B , treated as free parameters:

$$R(\tau) = \omega_A G_A(\tau) + \omega_B G_B(\tau) + (1 - \omega_A - \omega_B) G_C(\tau).$$

Based on MC studies with fully simulated signal samples, the means of the three Gaussian functions are fixed to zero, and the widths are linked by $\sigma_B = 2\sigma_A$ and $\sigma_C = 4\sigma_A$, where $\sigma_A = 0.04$ ps is fixed to the smallest value found in test fits.

The parameterisations of the functions $f_i(m_{\mu\mu})$ and $h_i(\tau)$ are summarised in Table 1. The mass lineshapes of the J/ψ and $\psi(2S)$ peaks, $f_i(m_{\mu\mu})$ for $i = 1$ to 4, are parameterised as weighted sums of two Gaussian functions and

a Crystal Ball function [41], which are the same for the prompt and non-prompt components. Based on MC studies, the weights are common to J/ψ and $\psi(2S)$, while the ratios of the peak positions and the widths are fixed to the ratio β of the masses [42] of the two states. Parameters of the Crystal Ball function were kept the same for both prompt and non-prompt J/ψ and also $\psi(2S)$, as verified from the MC studies. The lifetime distributions $h_1(\tau)$ and $h_3(\tau)$ of prompt J/ψ and $\psi(2S)$, respectively, are parameterised as delta functions, while for non-prompt $\psi(2S)$, a single-sided exponential function is used for $h_4(\tau)$. Since the non-prompt J/ψ sample is larger and has a wider observed τ range, its decay time distribution $h_2(\tau)$ is described by a superposition of two single-sided exponential functions with slopes related by $\gamma_1 = b\gamma_2$, where the constant $b = 1.4$ is obtained from test fits using real data. All these exponential functions are convolved with the resolution function $R(\tau)$.

In the $i = 1$ term, describing the prompt J/ψ peak, the product of the narrowest Gaussian term in $f_1(m_{\mu\mu})$ and the narrowest Gaussian term in $R(\tau)$ was replaced by a bivariate Gaussian function in $m_{\mu\mu}$ and τ with a correlation coefficient $\rho = 0.3$,

$$\begin{aligned} &\omega_0 G_1(m_{\mu\mu}; \sigma_1) \cdot f_A G_A(\tau; \sigma_A) \\ &\mapsto \omega_0 f_A G_{\text{BV}}(m_{\mu\mu}, \tau; \sigma_1, \sigma_A, \rho), \end{aligned} \quad (4)$$

to take into account the observed correlation between the measured values of these quantities. The effect of this correlation was found to be negligible for other terms.

Parameterisations for the background terms are selected using both the experience gained from similar analyses at lower energies [4] and physics considerations. In the prompt background term, $i = 5$, the mass distribution is modelled by a second-order polynomial, while the non-prompt mass distributions for $i = 6$ and 7 are parameterised as exponential functions, with independent parameters. The decay time distribution is a delta function for the prompt term $i = 5$, a single-sided exponential function for the main non-prompt term $i = 6$, and a symmetric double-sided exponential function for the last term, $i = 7$. Each of these is also convolved with the decay time resolution function $R(\tau)$.

Fits are performed in each (sub-)bin using an unbinned maximum-likelihood method, in the dimuon mass range from 2.7 to 4.1 GeV and the decay time range between -1 and 11 ps. Twenty of the 29 parameters are determined from the fit, with the rest fixed to predetermined values obtained from test fits using samples of MC simulated J/ψ and $\psi(2S)$ signal events. Uncertainties due to variations of the fit model and assumptions about the fixed parameters are estimated during the studies of systematic uncertainties described in Sect. 4. In particular, it is found that a reliable determination of the cross-sections for prompt and non-prompt production of the $\psi(2S)$ meson (with significance better than 5σ) is only

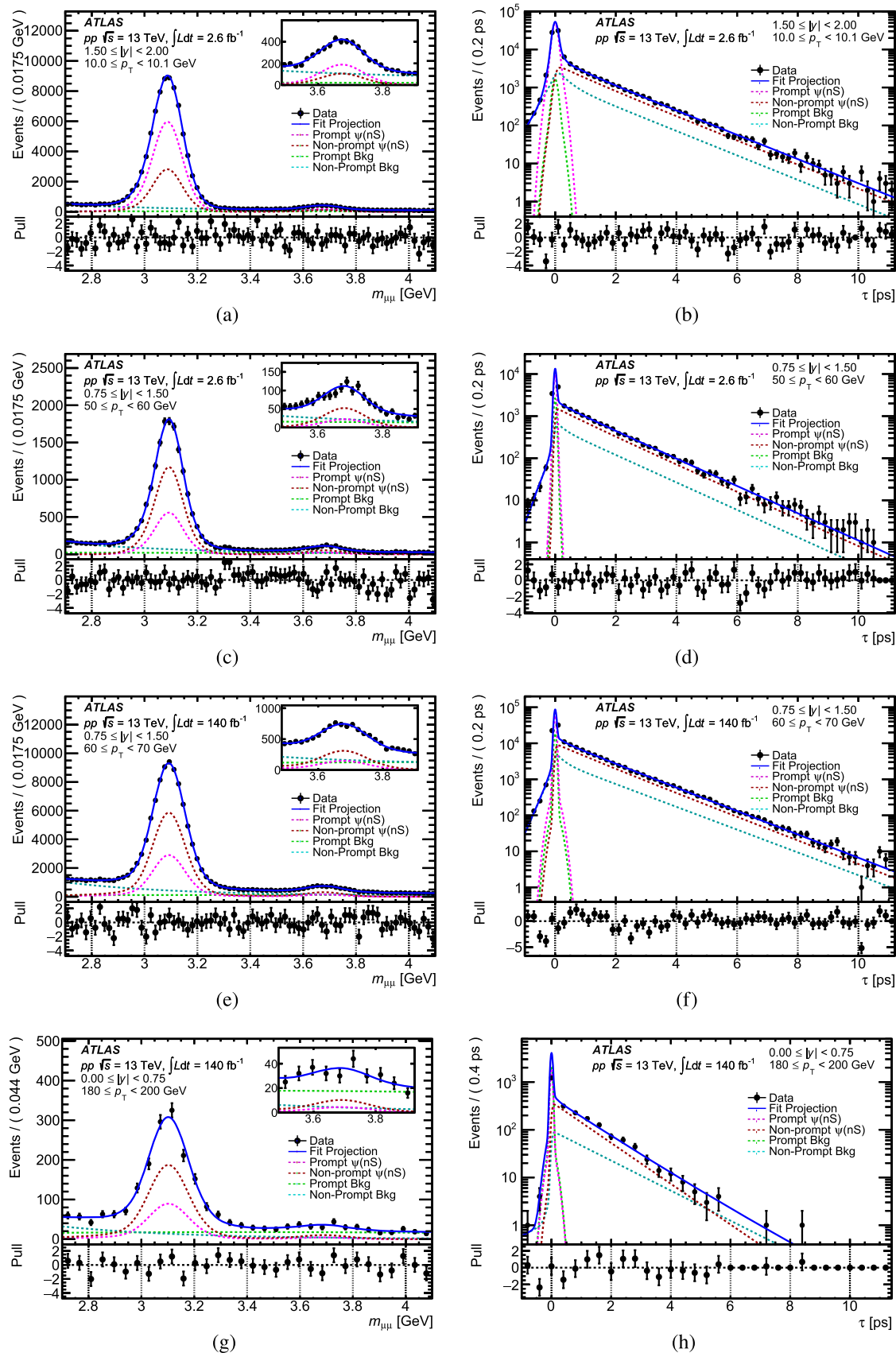


Fig. 1 Mass (left) and pseudo-proper decay time (right) projections of the fit result for selected analysis (sub-)bins. The values of $\chi^2/\text{d.o.f.}$ for the corresponding 2-dimensional fits are, from top to bottom: 1.09, 0.89, 1.20 and 0.93

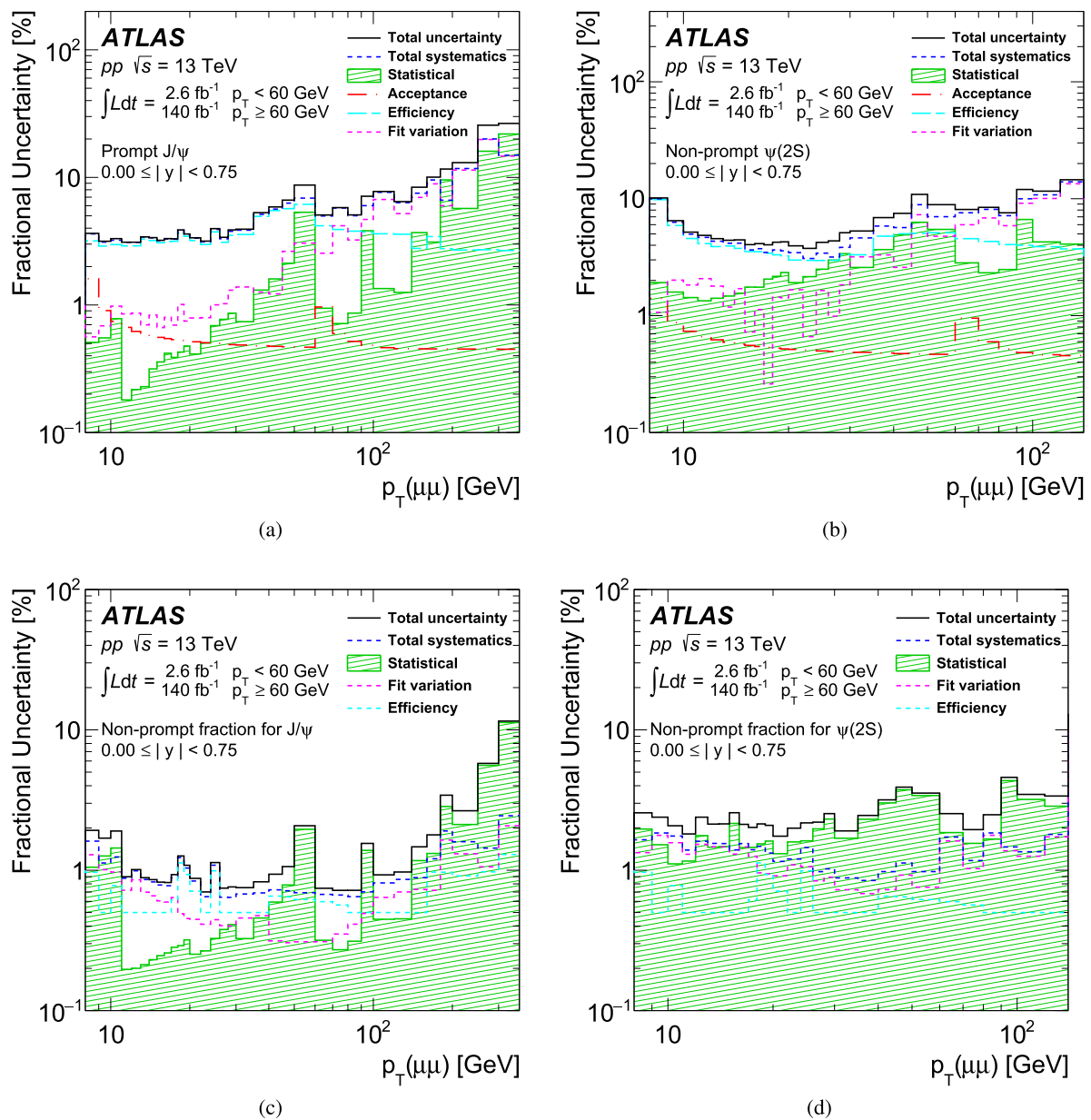


Fig. 2 Total, statistical, and systematic uncertainties (in %) as functions of p_T for the differential **a** prompt J/ψ and **b** non-prompt $\psi(2S)$ cross-sections, and for the non-prompt fractions of **c** J/ψ and **d** $\psi(2S)$,

in the rapidity slice $0.00 \leq |y| < 0.75$. The main components of the systematic uncertainties are also shown

possible up to $p_T = 140$ GeV, mainly due to poorer mass resolution and a lower signal-to-background ratio at higher p_T . For $p_T > 140$ GeV the yield of $\psi(2S)$ was fixed to a constant fraction (0.07) of the yield of J/ψ , by extrapolating the results from the fits at lower transverse momenta.

Figure 1 shows the mass and pseudo-proper decay time projections of the fits in several sample bins, together with the associated pull distributions. The quality of the fits, assessed by calculating a two-dimensional χ^2 value, is found to be good in all (sub-)bins.

The main parameters determined from the fits are the prompt and non-prompt yields of J/ψ and $\psi(2S)$ states. The cross-sections, non-prompt fractions and production ratios were then calculated using Eqs. (1)–(3), taking into account correlations between fit parameters. The results for all measured quantities are presented in Sect. 5.

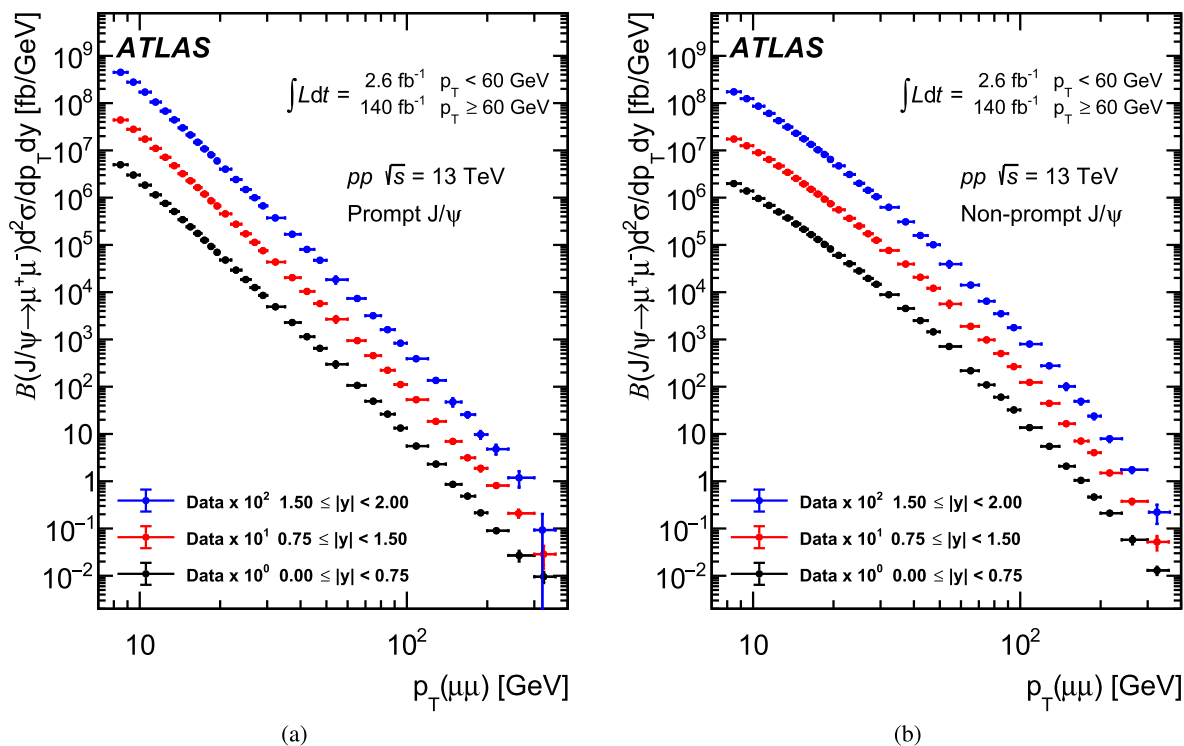


Fig. 3 Differential cross-sections for **a** prompt and **b** non-prompt production of J/ψ mesons. For visual clarity, a scaling factor of 1, 10, or 100 is applied to the rapidity slices $0.00 \leq |y| < 0.75$, $0.75 \leq |y| < 1.5$, and $1.5 \leq |y| < 2.0$, respectively. For each data point, the horizontal bar spans the p_T range covered by that bin, with the horizontal position of each point representing the mean p_T in that

bin. The vertical uncertainty range (obscured by the marker for some values) combines both the statistical (the inner bar) and total uncertainty. Uncertainties related to spin alignment or integrated luminosity are not included. Data up to 60 GeV were taken with a dimuon trigger with integrated luminosity 2.6 fb^{-1} ; data above 60 GeV were taken with a single-muon trigger with integrated luminosity 140 fb^{-1}

3.4 Efficiency corrections

As shown in Eq. (1), the yields obtained from two-dimensional maximum-likelihood fits in each (sub-)bin are subject to acceptance corrections, followed by the corrections for reconstruction and trigger efficiencies obtained from J/ψ and $\psi(2S)$ MC simulations, and by the correction scale factors that account for differences between data and MC simulation.

MC samples used for efficiency determinations were produced either by the PYTHIA 8 generator [43] with the A14 set of tuned parameters [44], or by a custom particle gun generator producing single ψ states with a given distribution, followed by their decay into a dimuon final state. The generated events were passed through the full ATLAS detector simulation [45] based on GEANT4 [46], and were reconstructed using the same software as the real data. The reconstruction efficiency ϵ_{reco} in each analysis (sub-)bin is defined as the ratio

$$\epsilon_{\text{reco}} = \frac{N_{\text{reco}}}{N_{\text{true}}},$$

where N_{reco} is the reconstructed yield within the bin boundaries defined in terms of reconstructed variables, with fiducial cuts applied to reconstructed variables, while N_{true} is the true (generated) yield within the bin boundaries defined in terms of true variable values, with fiducial cuts applied to the true variable values. This definition takes into account detector resolution smearing of the kinematic variables used to define the fiducial cuts and bin boundaries, and hence includes bin migration effects between neighbouring bins.

The trigger efficiency ϵ_{trig} , also obtained using MC simulations, is defined fully in terms of reconstructed variables as

$$\epsilon_{\text{trig}} = \frac{N_{\text{trig}}}{N_{\text{reco}}},$$

where N_{trig} is the number of triggered events among the reconstructed events. Since this measurement used two different triggers, the trigger efficiency was calculated accordingly. Further correction scale factors, ϵ_{recoSF} and ϵ_{trigSF} , are applied to account for any differences between data and MC events at reconstruction level and trigger level (see Eq. (1)). These are evaluated in dedicated tag-and-probe studies with

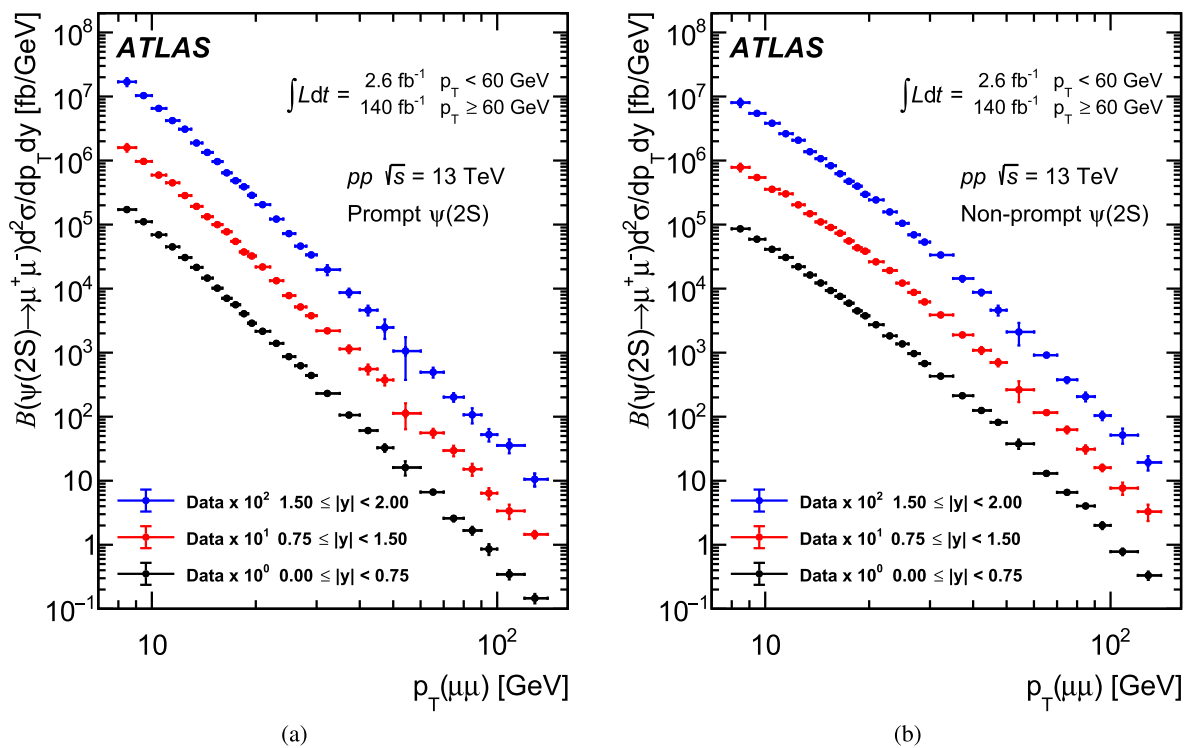


Fig. 4 Differential cross-sections for **a** prompt and **b** non-prompt production of $\psi(2S)$ mesons. For visual clarity, a scaling factor of 1, 10, or 100 is applied to the rapidity slices $0.00 \leq |y| < 0.75$, $0.75 \leq |y| < 1.5$, and $1.5 \leq |y| < 2.0$, respectively. For each data point, the horizontal bar spans the p_T range covered by that bin, with the horizontal position of each point representing the mean p_T in that

bin. The vertical uncertainty range (obscured by the marker for some values) combines both the statistical (the inner bar) and total uncertainty. Uncertainties related to spin alignment or integrated luminosity are not included. Data up to 60 GeV were taken with a dimuon trigger with integrated luminosity 2.6 fb^{-1} ; data above 60 GeV were taken with a single-muon trigger with integrated luminosity 140 fb^{-1}

auxiliary triggers, using a mixture of $J/\psi \rightarrow \mu^+\mu^-$ and $Z \rightarrow \mu^+\mu^-$ decays (see Ref. [40] for details).

4 Systematic uncertainties

Systematic effects from a variety of sources were studied, and appropriate corrections and uncertainties were assigned to all measured quantities. The systematic uncertainties can be broadly grouped into those related to reconstruction, trigger, and acceptance corrections, and those related to the fit model.

In order to assess the systematic uncertainties related to the fit model, the fit model was varied in several ways. As mentioned in Sect. 3.3, in the nominal fits some of the parameters describing the lineshapes of the signal peaks in the mass and lifetime domains were fixed to the values obtained from signal MC studies. These include the values of parameters α and n of the Crystal Ball function, the constant β linking the positions of the J/ψ and $\psi(2S)$ mass peaks, and the factor b relating the slopes of the two exponential functions describing the distribution of J/ψ decay times, τ . These parameters were allowed to float, one at a time, and the fits were repeated.

Some variations covered changes in the decay time resolution parameterisation, with widths of the three Gaussian functions changed independently. In other variations, alternative parameterisations were chosen for the mass dependence of the background terms, and the fits were repeated. In one of the variations the correlation parameter ρ from Eq. 4 was set to 0. Finally, in the highest p_T bins, $p_T > 140 \text{ GeV}$, the fixed fraction 0.07, relating the $\psi(2S)$ and J/ψ yields, was varied by 0.01 to cover the observed range at lower p_T values, and the fits were run again. After each rerun, changes in the measured yields were recorded. The outcome of this process, in each analysis bin, was a number of measurements of each yield, scattered around the result of the nominal fit for that yield. It was assumed that the probability distribution of these variations around the nominal value was uniform between the smallest and largest measured values, and, therefore, the corresponding systematic uncertainty was evaluated as the standard deviation of this uniform distribution.

Acceptance-related systematic uncertainties are governed by the size of the samples used to generate the corresponding acceptance maps. The chosen size ensured that these uncertainties are small relative to the total systematic uncertain-

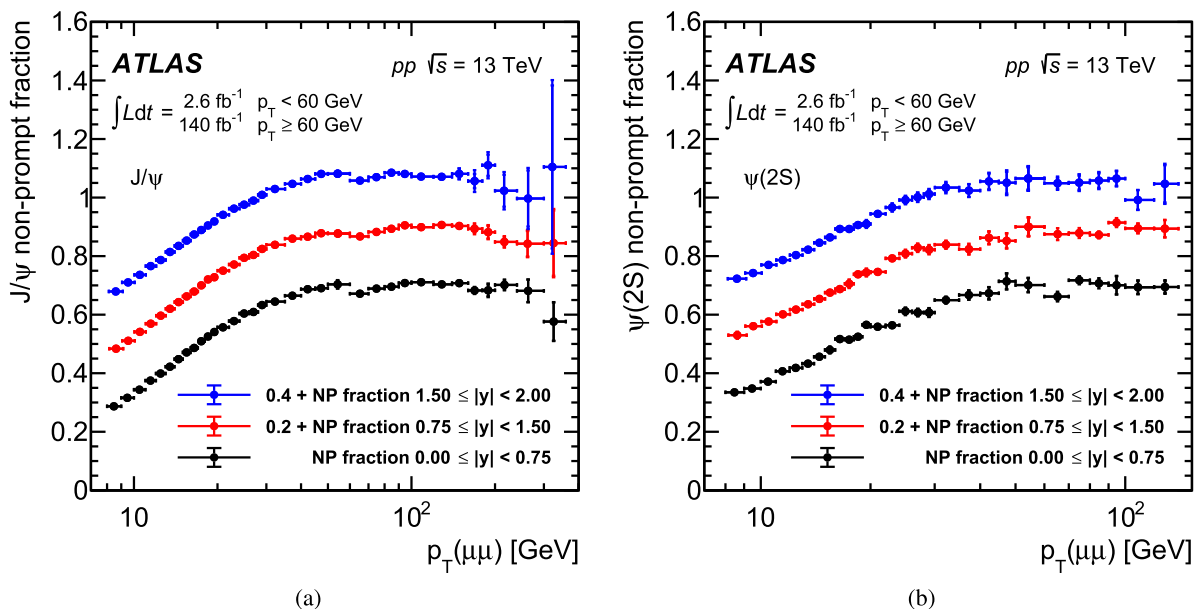


Fig. 5 Non-prompt production fraction of **a** J/ψ and **b** $\psi(2S)$ mesons. For visual clarity, a vertical shift of 0, 0.2, or 0.4 is applied to the rapidity slices $0.00 \leq |y| < 0.75$, $0.75 \leq |y| < 1.50$, and $1.5 \leq |y| < 2.0$, respectively. For each data point, the horizontal bar spans the p_T range covered by that bin, with the horizontal position of each point representing the mean p_T in that bin. The vertical uncertainty range (obscured

by the marker for some values) combines both the statistical (the inner bar) and total uncertainty. Uncertainties related to spin alignment or integrated luminosity are not included. Data up to 60 GeV were taken with a dimuon trigger with integrated luminosity 2.6 fb^{-1} ; data above 60 GeV were taken with a single-muon trigger with integrated luminosity 140 fb^{-1}

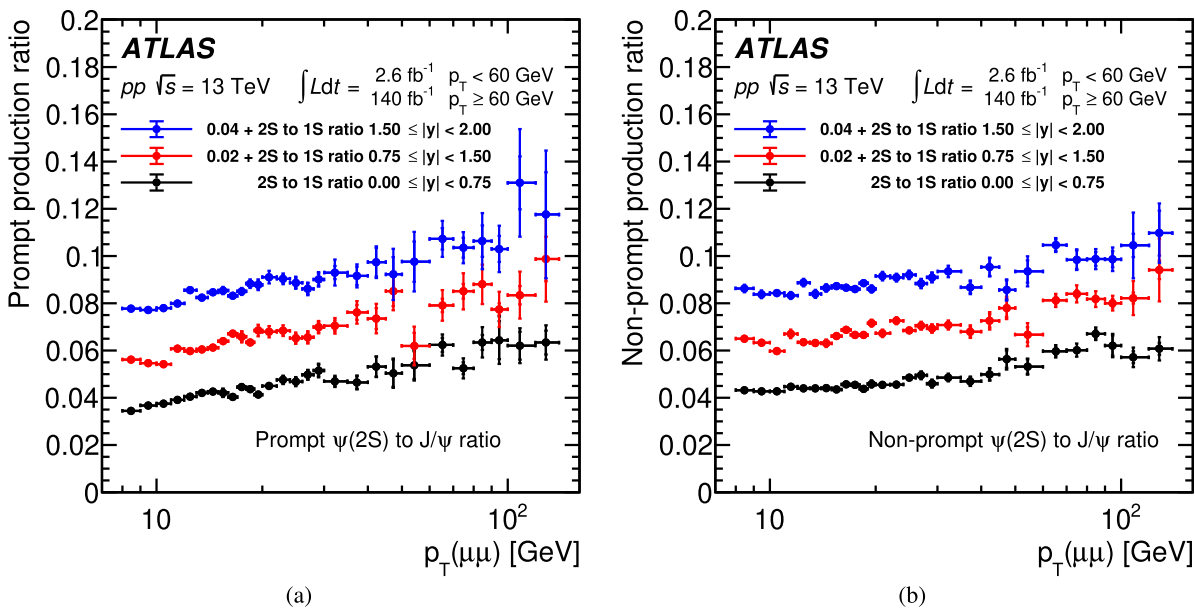


Fig. 6 The $\psi(2S)$ -to- J/ψ production ratio for the **a** prompt and **b** non-prompt production mechanisms. For visual clarity, a vertical shift of 0, 0.02, or 0.04 is applied to the rapidity slices $0.00 \leq |y| < 0.75$, $0.75 \leq |y| < 1.50$, and $1.5 \leq |y| < 2.0$, respectively. For each data point, the horizontal bar spans the p_T range covered by that bin, with the horizontal position of each point representing the mean p_T in that

bin. The vertical uncertainty range (hidden by the marker for some values) combines both the statistical (the inner bar) and total uncertainty. Uncertainties related to spin alignment or integrated luminosity are not included. Data up to 60 GeV were taken with a dimuon trigger with integrated luminosity 2.6 fb^{-1} ; data above 60 GeV were taken with a single-muon trigger with integrated luminosity 140 fb^{-1}

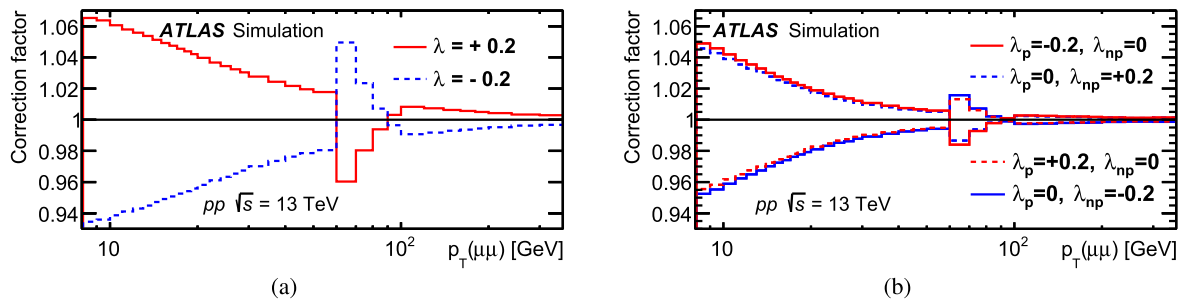


Fig. 7 Spin-alignment hypothesis correction factors for the J/ψ **a** differential cross-section and **b** non-prompt production fraction, for a number of spin-alignment scenarios. The correction factors are approximately the same for J/ψ and $\psi(2S)$, for the prompt and non-prompt

production mechanisms, and also for the three rapidity regions. The discontinuities at $p_T = 60$ GeV are due to the transition from a low- p_T dimuon trigger to a high- p_T single-muon trigger, and the corresponding change in event acceptance

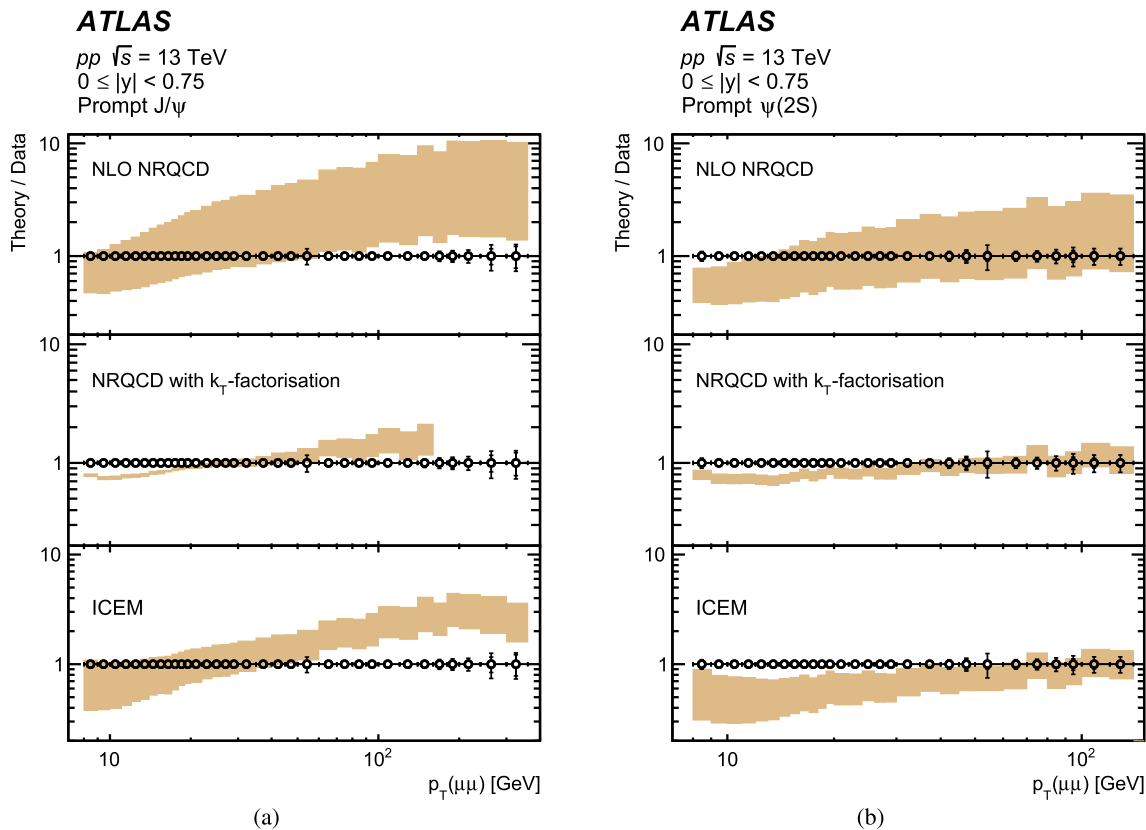


Fig. 8 Ratios of various theoretical predictions (described in the text) to the data points from this measurement, for the prompt production of **a** J/ψ and **b** $\psi(2S)$ in the central rapidity region. In each p_T bin, the shaded area represents the ratio of the theoretical prediction to the

measured value, with the vertical spread showing the uncertainties of the respective model. Error bars on the black circles show fractional uncertainties of this measurement

ties. Changes in acceptance due to different spin-alignment hypotheses were treated separately (see Appendix).

Systematic uncertainties due to trigger and reconstruction efficiency corrections include the uncertainties on the scale factors [40] as well as those due the sizes and shapes of the MC samples. These were added in quadrature.

The total systematic uncertainty in each bin is calculated by summing in quadrature the uncertainties from the above-mentioned sources. The total uncertainty is calculated as the sum in quadrature of the total systematic and statistical uncertainties.

An additional systematic uncertainty comes from the determination of the integrated luminosity. In the $p_T <$

60 GeV region, where only 2015 data contributes to this measurement, the integrated luminosity has a 1.13% uncertainty [47], while for $p_T \geq 60$ GeV the uncertainty in the combined 2015–2018 integrated luminosity is 0.83%, as obtained using the LUCID-2 detector [48].

As an illustration, in Fig. 2 the total, statistical, and systematic uncertainties, together with the main individual contributions to the systematic uncertainty, are shown for the central rapidity slice for the differential cross-sections of prompt J/ψ and non-prompt $\psi(2S)$ mesons, as well as for the non-prompt fractions of J/ψ and $\psi(2S)$ mesons, as functions of p_T . For the cross-sections, apart from a few high p_T bins, the uncertainties are largely systematic, while for the non-prompt fractions and $\psi(2S)$ -to- J/ψ production ratios, statistical errors dominate in many bins because the systematic uncertainties partially cancel out. Error levels are similar between prompt and non-prompt cross sections. Comparable results are obtained in other rapidity slices.

5 Results

The measured double-differential cross-sections for prompt and non-prompt J/ψ production in the nominal isotropic spin-alignment scenario are presented in Fig. 3a b, respectively. The same quantities for $\psi(2S)$ are shown in Fig. 4a and b. The non-prompt production fractions for J/ψ and $\psi(2S)$ are presented in Fig. 5a and b. Finally, the $\psi(2S)$ -to- J/ψ production ratios are presented in Fig. 6a and b for the prompt and non-prompt production mechanisms, respectively.

While the non-prompt fractions shown in Fig. 5 increase steadily with p_T up to about 100 GeV, they are almost constant for both J/ψ and $\psi(2S)$ in the high p_T range, which suggests similar p_T -dependences for the prompt and non-prompt differential cross-sections at very high transverse momenta.

5.1 Acceptance and spin alignment corrections

The transition between the low- p_T dimuon trigger and the high- p_T single-muon trigger at $p_T = 60$ GeV presents a particular challenge because of the sharp change in event kinematics. The corresponding changes in the acceptance and efficiency correction factors are significant and could lead to discontinuities in the measured distributions.

Since the spin alignment of ψ states may be different for the prompt and non-prompt production mechanisms, additional correction factors may be needed for all measured distributions. In order to quantitatively assess the possible impact of ψ spin alignment, correction factors are calculated for a variety of scenarios. It was found that the dependence on the polar angle θ in the helicity frame of the ψ state

causes the largest variation, so the angular dependence of $\psi \rightarrow \mu^+\mu^-$ decays is assumed to be $\propto (1 + \lambda_\theta \cos^2 \theta)$. The correction factors are shown in Fig. 7a and b for the differential cross-sections and non-prompt fractions respectively, where the values $\lambda_\theta = \pm 0.20$ are chosen to reflect the approximate level of experimental knowledge [7, 36, 49] and theoretical understanding [50–52] of this parameter. The correction factors are shown for prompt J/ψ in the central rapidity range, but were found to be essentially the same for J/ψ and $\psi(2S)$, for the prompt and non-prompt production mechanisms, and also for the three rapidity regions.

The potential bias due to the spin-alignment assumption is especially noticeable at the $p_T = 60$ GeV transition, and indeed a step can be seen at this point in the J/ψ non-prompt fraction in Fig. 5a, reflecting a possible issue in the spin-alignment modelling. Correction factors for some other values of λ_θ are presented in the Appendix. These can be used for further studies, if more precise spin-alignment data and/or improved modelling become available in the future.

5.2 Theory comparison: prompt production

Model calculations of prompt production of charmonium are usually based on perturbative QCD for the production of the $c\bar{c}$ pair, and differ in the mechanism of hadronisation and formation of the bound state with specific quantum numbers.

The predictions of a model using the non-relativistic QCD approach to charmonium production cross-sections at next-to-leading order (NLO NRQCD) [53], using predetermined LDMEs [54, 55], are shown in comparison with our measurements of the J/ψ and $\psi(2S)$ production cross-sections in the top panels of Fig. 8a and b respectively. The predictions of the model largely overlap with the data points within the theoretical uncertainties, which include variations of the renormalisation, factorisation and NRQCD scales. However, the predictions seem to overestimate the cross-sections at high p_T .

One generalisation of the NRQCD approach is a model which aims to improve the description by taking into account the transverse degrees of freedom of the initial gluons in the colliding protons (k_T -factorisation model) [56, 57]. The predictions of this model, obtained with the PEGASUS event generator [58] using the LDMEs determined in Ref. [59], are compared with our measured results as shown in the middle panels of Fig. 8a and b for J/ψ and $\psi(2S)$ respectively, where the theoretical uncertainties only account for variations of the renormalisation scale. The predictions of the model tend to underestimate the cross-sections at low p_T , while in the high p_T region the range of comparison is limited by the availability of the transverse-momentum-dependent parton distribution function (PDF) of the gluon [60].

A different approach is used by the Improved Colour Evaporation Model (ICEM) [61], which assigns a fixed frac-

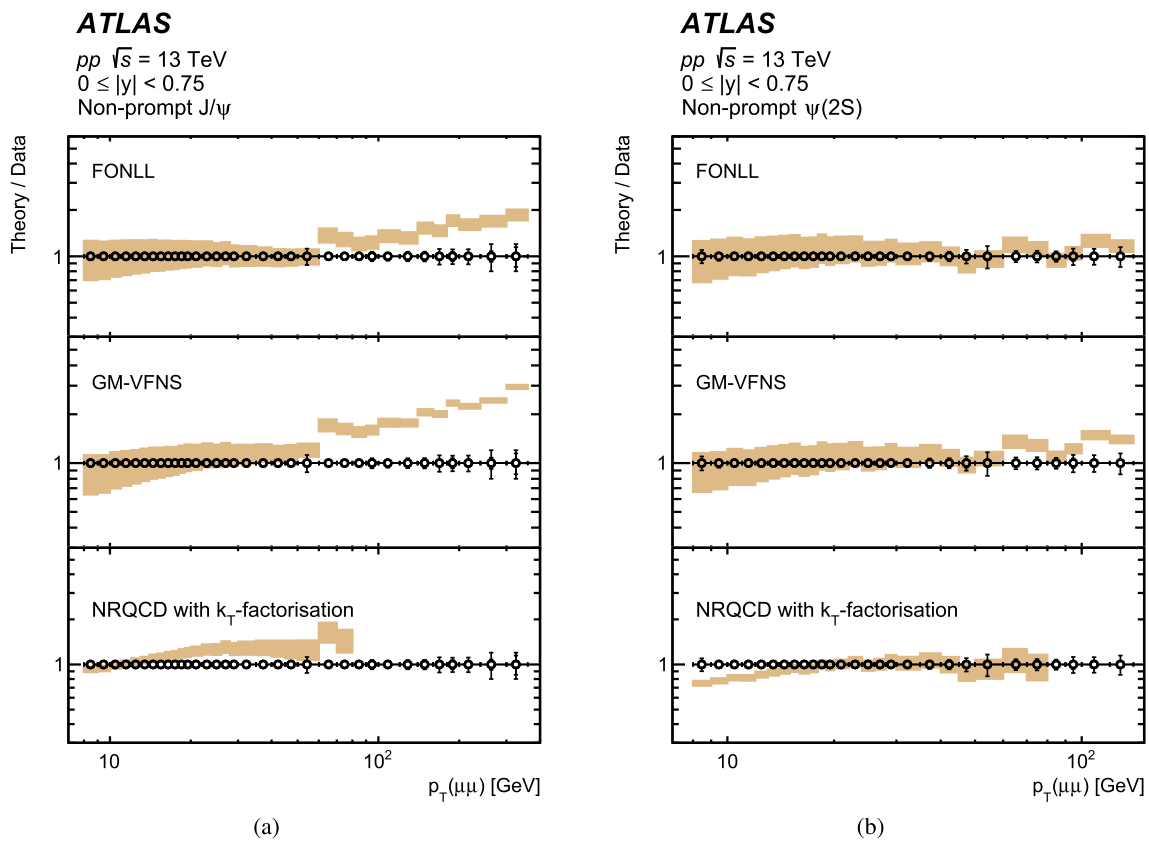


Fig. 9 Ratios of various theoretical predictions (described in the text) to the data points from this measurement, for non-prompt production of **a** J/ψ and **b** $\psi(2S)$ in the central rapidity region. In each p_T bin, the shaded area represents the ratio of the theoretical prediction to the

measured value, with the vertical spread showing the uncertainties of the respective model. Error bars on the black circles show fractional uncertainties of this measurement

tion of the $c\bar{c}$ production cross-section below the open charm threshold to individual charmonium states. Comparisons of ICeM predictions with the parameter values and their uncertainties previously determined from fits to LHCb data at 7 TeV [10, 62] are shown in the bottom panels of Fig. 8a and b for J/ψ and $\psi(2S)$ respectively. The model seems to predict somewhat harder p_T spectra than observed in the data for both J/ψ and $\psi(2S)$, and tends to underestimate the cross-section for $\psi(2S)$.

5.3 Theory comparison: non-prompt production

Theoretical calculations of non-prompt charmonium production are based on perturbative QCD for the production of a $b\bar{b}$ quark pair, their hadronisation into a pair of b -hadrons, and their subsequent decay into a charmonium state with specific quantum numbers. Predictions from one such model, based on fixed-order-next-to-leading-log (FONLL) QCD calculations [1, 2] were obtained using the web-based tool [63] with default parameter values, and are shown in comparison with our measurements in the top panels of Fig. 9a and b for

J/ψ and $\psi(2S)$ respectively. Here the uncertainties cover variations of both the renormalisation scale and the charm quark mass. Agreement is good at lower p_T values, but the FONLL model predicts higher cross-sections for J/ψ at the high p_T end.

Another set of predictions, based on the next-to-leading-order QCD calculation in the general-mass-variable-flavour-number scheme (GM-VFNS) [64] are shown in the middle panels of Fig. 9a and b. Parameter values were determined in Ref. [54, 65], with uncertainties originating from renormalisation scale dependence. These predictions lead to similar results, but the deviation from data at the highest p_T values is somewhat more pronounced, especially in the J/ψ case.

Finally, the NRQCD model with k_T -factorisation can also be used to predict the p_T distributions of vector charmonia through the non-prompt production mechanisms [58, 66] (see bottom panels of Fig. 9a and b). Where available, the shapes of p_T distributions are reproduced fairly well for both J/ψ and $\psi(2S)$, but the limitations of the transverse-momentum-dependent model for the gluon PDF show up at even lower charmonium p_T values. Also, in this model the

cross-section for $\psi(2S)$ non-prompt production at low p_T is somewhat underestimated.

Overall, none of the models considered here is able to describe the data over the whole measured range of transverse momenta. The general trend shown by all theoretical models is a slower-than-observed decrease of the cross-section with p_T , which could be related to insufficiently accounting for PDF evolution and/or possible dependence of LDMEs on transverse momentum. In any case, these measurements should help refine theoretical models of hadronic production of quarkonium at the highest available energies and at transverse momenta well beyond 100 GeV.

6 Summary

This paper describes a measurement of the double-differential production cross-sections of J/ψ and $\psi(2S)$ charmonium states in pp collisions at $\sqrt{s} = 13$ TeV, performed through their decays into dimuons and using 140 fb^{-1} of data collected by the ATLAS detector at the LHC during Run 2. The cross-sections for each of the two states are measured separately for prompt and non-prompt production mechanisms. The non-prompt fractions for each state are also measured, along with the $\psi(2S)$ -to- J/ψ production ratios. The rapidity range of the measurement is $|y| < 2$. For $\psi(2S)$ meson the transverse momentum range is 8–140 GeV, while for J/ψ state the results cover a much wider transverse momentum range, from 8 to 360 GeV, extending well beyond the range of previous measurements. In the high p_T range the results show similar p_T -dependences for the prompt and non-prompt differential cross-sections, with the non-prompt fractions being nearly constant for both J/ψ and $\psi(2S)$ states.

The results are compared with a number of theoretical predictions, which describe the data with varying degrees of success. The extended p_T reach of this measurement provides important fresh input for future tuning of theoretical models.

Acknowledgements We thank CERN for the very successful operation of the LHC, as well as the support staff from our institutions without whom ATLAS could not be operated efficiently. We acknowledge the support of ANPCyT, Argentina; YerPhI, Armenia; ARC, Australia; BMWFW and FWF, Austria; ANAS, Azerbaijan; CNPq and FAPESP, Brazil; NSERC, NRC and CFI, Canada; CERN; ANID, Chile; CAS, MOST and NSFC, China; Minciencias, Colombia; MEYS CR, Czech Republic; DNRF and DNSRC, Denmark; IN2P3-CNRS and CEA-DRF/IRFU, France; SRNSFG, Georgia; BMBF, HGF and MPG, Germany; GSRI, Greece; RGC and Hong Kong SAR, China; ISF and Benozziyo Center, Israel; INFN, Italy; MEXT and JSPS, Japan; CNRST, Morocco; NWO, Netherlands; RCN, Norway; MEiN, Poland; FCT, Portugal; MNE/IFA, Romania; MESTD, Serbia; MSSR, Slovakia; ARRS and MIZŠ, Slovenia; DSI/NRF, South Africa; MICINN, Spain; SRC and Wallenberg Foundation, Sweden; SERI, SNSF and Cantons of Bern and Geneva, Switzerland; MOST, Taipei; TENMAK, Türkiye; STFC, United Kingdom; DOE and NSF, United States of America. In addition, individual groups and members have received support from BCKDF,

CANARIE, CRC and DRAC, Canada; PRIMUS 21/SCI/017 and UNCE SCI/013, Czech Republic; COST, ERC, ERDF, Horizon 2020, ICSC-NextGenerationEU and Marie Skłodowska-Curie Actions, European Union; Investissements d’Avenir Labex, Investissements d’Avenir Idex and ANR, France; DFG and AvH Foundation, Germany; Herakleitos, Thales and Aristeia programmes co-financed by EU-ESF and the Greek NSRF, Greece; BSF-NSF and MINERVA, Israel; Norwegian Financial Mechanism 2014–2021, Norway; NCN and NAWA, Poland; La Caixa Banking Foundation, CERCA Programme Generalitat de Catalunya and PROMETEO and GenT Programmes Generalitat Valenciana, Spain; Göran Gustafssons Stiftelse, Sweden; The Royal Society and Leverhulme Trust, United Kingdom. The crucial computing support from all WLCG partners is acknowledged gratefully, in particular from CERN, the ATLAS Tier-1 facilities at TRIUMF/SFU (Canada), NDGF (Denmark, Norway, Sweden), CC-IN2P3 (France), KIT/GridKA (Germany), INFN-CNAF (Italy), NL-T1 (Netherlands), PIC (Spain), RAL (UK) and BNL (USA), the Tier-2 facilities worldwide and large non-WLCG resource providers. Major contributors of computing resources are listed in Ref. [67].

Data Availability Statement This manuscript has no associated data or the data will not be deposited. [Authors’ comment: The experimental data that support the findings of this study are available in HEPData at the following link <https://www.hepdata.net/record/145071>.]

Open Access This article is licensed under a Creative Commons Attribution 4.0 International License, which permits use, sharing, adaptation, distribution and reproduction in any medium or format, as long as you give appropriate credit to the original author(s) and the source, provide a link to the Creative Commons licence, and indicate if changes were made. The images or other third party material in this article are included in the article’s Creative Commons licence, unless indicated otherwise in a credit line to the material. If material is not included in the article’s Creative Commons licence and your intended use is not permitted by statutory regulation or exceeds the permitted use, you will need to obtain permission directly from the copyright holder. To view a copy of this licence, visit <http://creativecommons.org/licenses/by/4.0/>. Funded by SCOAP³.

Appendix

The ψ meson’s acceptance depends on its spin alignment. The nominal results presented in this paper assume an isotropic angular distribution, corresponding to the “unpolarised” case. In order to assess the dependence of the cross-section on the spin alignment, the acceptance maps were reweighted for a variety of spin-alignment scenarios, and for each analysis bin the correction factors were determined relative to the nominal values. The correction factors calculated for several values of the parameter λ_θ , assuming the angular dependence in the ψ helicity frame to be $\propto (1 + \lambda_\theta \cos^2 \theta)$, are shown in Table 2. The factors are shown for prompt J/ψ in the central rapidity range, but were found to be the same for J/ψ and $\psi(2S)$ within 1–2%, with the variation over the other rapidity ranges also within 1–2%. For $\lambda_\theta \neq 0$ the nominal value of the measured cross-section should be multiplied by the appropriate correction factor from Table 2.

Table 2 Correction factors for an assumed angular dependence $\propto 1 + \lambda_\theta \cos^2 \theta$ in the helicity frame, for several values of the parameter λ_θ . The correction factors were found to be the same (within 1–2%) for J/ψ and $\psi(2S)$ mesons, for prompt and non-prompt production mechanisms, and for the three rapidity intervals considered in this paper

p_T	$\lambda_\theta = -1$	$\lambda_\theta = -0.2$	$\lambda_\theta = +0.2$	$\lambda_\theta = +1$
8–9 [GeV]	0.69	0.93	1.07	1.29
9–10 [GeV]	0.69	0.94	1.06	1.28
10–11 [GeV]	0.70	0.94	1.06	1.27
11–12 [GeV]	0.70	0.94	1.06	1.26
12–13 [GeV]	0.71	0.94	1.06	1.25
13–14 [GeV]	0.72	0.94	1.05	1.24
14–15 [GeV]	0.73	0.95	1.05	1.24
15–16 [GeV]	0.73	0.95	1.05	1.22
16–17 [GeV]	0.74	0.95	1.05	1.21
17–18 [GeV]	0.75	0.95	1.05	1.20
18–19 [GeV]	0.75	0.95	1.04	1.20
19–20 [GeV]	0.76	0.96	1.04	1.19
20–22 [GeV]	0.77	0.96	1.04	1.18
22–24 [GeV]	0.78	0.96	1.04	1.17
24–26 [GeV]	0.79	0.96	1.03	1.15
26–28 [GeV]	0.80	0.97	1.03	1.14
28–30 [GeV]	0.81	0.97	1.03	1.13
30–35 [GeV]	0.82	0.97	1.03	1.12
35–40 [GeV]	0.84	0.97	1.02	1.10
40–45 [GeV]	0.86	0.98	1.02	1.09
45–50 [GeV]	0.87	0.98	1.02	1.08
50–60 [GeV]	0.88	0.98	1.02	1.07
60–70 [GeV]	1.48	1.05	0.96	0.86
70–80 [GeV]	1.19	1.02	0.98	0.93
80–90 [GeV]	1.05	1.01	0.99	0.98
90–100 [GeV]	0.98	1.00	1.00	1.01
100–120 [GeV]	0.94	0.99	1.01	1.03
120–140 [GeV]	0.94	0.99	1.01	1.03
140–160 [GeV]	0.95	0.99	1.01	1.03
160–180 [GeV]	0.96	0.99	1.01	1.02
180–200 [GeV]	0.96	0.99	1.00	1.02
200–240 [GeV]	0.97	1.00	1.00	1.02
240–300 [GeV]	0.97	1.00	1.00	1.01
300–360 [GeV]	0.98	1.00	1.00	1.01

References

- M. Cacciari, S. Frixione, P. Nason, The p_T spectrum in heavy flavor photoproduction. *JHEP* **03**, 006 (2001). <https://doi.org/10.1088/1126-6708/2001/03/006>. arXiv:0102134 [hep-ph]
- M. Cacciari et al., Theoretical predictions for charm and bottom production at the LHC. *JHEP* **10**, 137 (2012). [https://doi.org/10.1007/JHEP10\(2012\)137](https://doi.org/10.1007/JHEP10(2012)137). arXiv:1205.6344
- G.-T. Bodwin, E. Braaten, G.-P. Lepage, Rigorous QCD analysis of inclusive annihilation and production of heavy quarkonium. *Phys. Rev. D* **51**, 1125 (1995). <https://doi.org/10.1103/PhysRevD.51.1125>. arXiv:9407339 [hep-ph]. [Erratum: *Phys. Rev. D* **55** (1997)]
- ATLAS Collaboration, Measurement of the differential cross-sections of prompt and non-prompt production of J/ψ and $\psi(2S)$ in pp collisions at $\sqrt{s} = 7$ and 8 TeV with the ATLAS detector. *Eur. Phys. J. C* **76**, 283 (2016). <https://doi.org/10.1140/epjcs/10052-016-4050-8>. arXiv:1512.03657
- ATLAS Collaboration, Measurement of the production cross-section of $\psi(2S) \rightarrow J/\psi(\rightarrow \mu^+\mu^-)\pi^+\pi^-$ in pp collisions at $\sqrt{s} = 7$ TeV at ATLAS. *JHEP* **09**, 079 (2014). [https://doi.org/10.1007/JHEP09\(2014\)079](https://doi.org/10.1007/JHEP09(2014)079). arXiv:1407.5532
- LHCb Collaboration, Measurement of $\psi(2S)$ meson production in pp collisions at $\sqrt{s} = 7$ TeV. *Eur. Phys. J. C* **72**, 2100 (2012). <https://doi.org/10.1140/epjcs/10052-012-2100-4>. arXiv:1204.1258
- CMS Collaboration, J/ψ and $\psi(2S)$ production in pp collisions at $\sqrt{s} = 7$ TeV. *JHEP* **02**, 011 (2012). [https://doi.org/10.1007/JHEP02\(2012\)011](https://doi.org/10.1007/JHEP02(2012)011). arXiv:1111.1557
- ALICE Collaboration, J/ψ polarization in pp collisions at $\sqrt{s} = 7$ TeV. *Phys. Rev. Lett.* **108**, 082001 (2012). <https://doi.org/10.1103/PhysRevLett.108.082001>. arXiv:1111.1630
- CMS Collaboration, Measurement of the prompt J/ψ and $\psi(2S)$ polarizations in pp collisions at $\sqrt{s} = 7$ TeV. *Phys. Lett. B* **727**, 381 (2013). <https://doi.org/10.1016/j.physletb.2013.10.055>. arXiv:1307.6070
- LHCb Collaboration, Measurement of $\psi(2S)$ polarisation in pp collisions at $\sqrt{s} = 7$ TeV. *Eur. Phys. J. C* **74**, 2872 (2014). <https://doi.org/10.1140/epjcs/10052-014-2872-9>. arXiv:1403.1339
- ALICE Collaboration, Measurement of the inclusive J/ψ polarization at forward rapidity in pp collisions at $\sqrt{s} = 8$ TeV. *Eur. Phys. J. C* **78**, 562 (2018). <https://doi.org/10.1140/epjcs/10052-018-6027-2>. arXiv:1805.04374
- ATLAS Collaboration, Measurement of the production cross section of prompt J/ψ mesons in association with a W^\pm boson in pp collisions at $\sqrt{s} = 7$ TeV with the ATLAS detector. *JHEP* **04**, 172 (2014). [https://doi.org/10.1007/JHEP04\(2014\)172](https://doi.org/10.1007/JHEP04(2014)172). arXiv:1401.2831
- ATLAS Collaboration, Observation and measurements of the production of prompt and non-prompt J/ψ mesons in association with a Z boson in pp collisions at $\sqrt{s} = 8$ TeV with the ATLAS detector. *Eur. Phys. J. C* **75**, 229 (2015). <https://doi.org/10.1140/epjcs/10052-015-3406-9>. arXiv:1412.6428
- G. Li, M. Song, R.-Y. Zhang, W.-G. Ma, QCD corrections to J/ψ production in association with a W -boson at the LHC. *Phys. Rev. D* **83**, 014001 (2011). <https://doi.org/10.1103/PhysRevD.83.014001>. arXiv:1012.3798
- J.-P. Lansberg, C. Lorce, Reassessing the importance of the colour-singlet contributions to direct $J/\psi + W$ production at the LHC and the Tevatron. *Phys. Lett. B* **726**, 218 (2013). <https://doi.org/10.1016/j.physletb.2013.07.059>. arXiv:1303.5327
- B. Gong, J.P. Lansberg, C. Lorce, J. Wang, Next-to-leading-order QCD corrections to the yields and polarisations of J/ψ and Υ directly produced in association with a Z boson at the LHC. *JHEP* **03**, 115 (2013). [https://doi.org/10.1007/JHEP03\(2013\)115](https://doi.org/10.1007/JHEP03(2013)115). arXiv:1210.2430
- M. Song, W.-G. Ma, G. Li, R.-Y. Zhang, L. Guo, QCD corrections to J/ψ plus Z^0 -boson production at the LHC. *JHEP* **02**, 071 (2011). [https://doi.org/10.1007/JHEP02\(2011\)071](https://doi.org/10.1007/JHEP02(2011)071). arXiv:1102.0398. [Erratum: *JHEP* **12**, 010 (2012)]
- M. Butenschoen, B.A. Kniehl, J/ψ production in NRQCD: a global analysis of yield and polarization. *Nucl. Phys. Proc. Suppl.* **222–224**, 151 (2012). <https://doi.org/10.1016/j.nuclphysbps.2012.03.016>. arXiv:1201.3862
- V.D. Barger, W.-Y. Keung, R.J.N. Phillips, On psi and upsilon production via gluons. *Phys. Lett. B* **91**, 253 (1980). [https://doi.org/10.1016/0370-2693\(80\)90444-X](https://doi.org/10.1016/0370-2693(80)90444-X)

20. V.D. Barger, W.-Y. Keung, R.J.N. Phillips, Hadroproduction of ψ and Υ . *Z. Phys. C* **6**, 169 (1980). <https://doi.org/10.1007/BF01588844>
21. R. Gavai et al., Quarkonium production in hadronic collisions. *Int. J. Mod. Phys. A* **10**, 3043 (1995). <https://doi.org/10.1142/S0217751X95001443>. arXiv:hep-ph/9502270
22. Y.-Q. Ma, R. Vogt, Quarkonium production in an improved color evaporation model. *Phys. Rev. D* **94**, 114029 (2016). <https://doi.org/10.1103/PhysRevD.94.114029>. arXiv:1609.06042
23. CMS Collaboration, Measurement of J/ψ and $\psi(2S)$ prompt double-differential cross sections in pp collisions at $\sqrt{s} = 7$ TeV. *Phys. Rev. Lett.* **114**, 191802 (2015). <https://doi.org/10.1103/PhysRevLett.114.191802>. arXiv:1502.04155
24. CMS Collaboration, Measurement of quarkonium production cross sections in pp collisions at $\sqrt{s} = 13$ TeV. *Phys. Lett. B* **780**, 251 (2018). <https://doi.org/10.1016/j.physletb.2018.02.033>. arXiv:1710.11002
25. LHCb Collaboration, Exclusive J/ψ and $\psi(2S)$ production in pp collisions at $\sqrt{s} = 7$ TeV. *J. Phys. G* **40**, 045001 (2013). <https://doi.org/10.1088/0954-3899/40/4/045001>. arXiv:1301.7084
26. LHCb Collaboration, Measurement of J/ψ polarization in pp collisions at $\sqrt{s} = 7$ TeV. *Eur. Phys. J. C* **73**, 2631 (2013). <https://doi.org/10.1140/epjc/s10052-013-2631-3>. arXiv:1307.6379
27. LHCb Collaboration, Updated measurements of exclusive J/ψ and $\psi(2S)$ production cross-sections in pp collisions at $\sqrt{s} = 7$ TeV. *J. Phys. G* **41**, 055002 (2014). <https://doi.org/10.1088/0954-3899/41/5/055002>. arXiv:1401.3288
28. LHCb Collaboration, Measurement of forward J/ψ production cross-sections in pp collisions at $\sqrt{s} = 13$ TeV. *JHEP* **10**, 172 (2015). [https://doi.org/10.1007/JHEP10\(2015\)172](https://doi.org/10.1007/JHEP10(2015)172). arXiv:1509.00771. [Erratum: *JHEP* **05**, 063 (2017)]
29. LHCb Collaboration, Central exclusive production of J/ψ and $\psi(2S)$ mesons in pp collisions at $\sqrt{s} = 13$ TeV. *JHEP* **10**, 167 (2018). [https://doi.org/10.1007/JHEP10\(2018\)167](https://doi.org/10.1007/JHEP10(2018)167). arXiv:1806.04079
30. ALICE Collaboration, Measurement of quarkonium production at forward rapidity in pp collisions at $\sqrt{s} = 7$ TeV. *Eur. Phys. J. C* **74**, 2974 (2014). <https://doi.org/10.1140/epjc/s10052-014-2974-4>. arXiv:1403.3648
31. ALICE Collaboration, Prompt and non-prompt J/ψ production cross sections at midrapidity in proton–proton collisions at $\sqrt{s} = 5.02$ and 13 TeV. *JHEP* **03**, 190 (2022). [https://doi.org/10.1007/JHEP03\(2022\)190](https://doi.org/10.1007/JHEP03(2022)190). arXiv:2108.02523
32. ALICE Collaboration, Prompt and non-prompt J/ψ production cross sections at midrapidity in proton–proton collisions at $\sqrt{s} = 5.02$ and 13 TeV. *JHEP* **03**, 190 (2022). [https://doi.org/10.1007/JHEP03\(2022\)190](https://doi.org/10.1007/JHEP03(2022)190). arXiv:2108.02523
33. ALICE Collaboration, Inclusive J/ψ production at midrapidity in pp collisions at $\sqrt{s} = 13$ TeV. *Eur. Phys. J. C* **81**, 1121 (2021). <https://doi.org/10.1140/epjc/s10052-021-09873-4>. arXiv:2108.01906
34. ALICE Collaboration, Energy dependence of forward-rapidity J/ψ and $\psi(2S)$ production in pp collisions at the LHC. *Eur. Phys. J. C* **77**, 392 (2017). <https://doi.org/10.1140/epjc/s10052-017-4940-4>. arXiv:1702.00557
35. ALICE Collaboration, Measurement of prompt J/ψ and beauty hadron production cross sections at mid-rapidity in pp collisions at $\sqrt{s} = 7$ TeV. *JHEP* **11**, 065 (2012). [https://doi.org/10.1007/JHEP11\(2012\)065](https://doi.org/10.1007/JHEP11(2012)065). arXiv:1205.5880
36. ALICE Collaboration, J/ψ polarization in pp collisions at $\sqrt{s} = 7$ TeV. *Phys. Rev. Lett.* **108**, 082001 (2012). <https://doi.org/10.1103/PhysRevLett.108.082001>. arXiv:1111.1630
37. ATLAS Collaboration, Measurement of χ_{c1} and χ_{c2} production with $\sqrt{s} = 7$ TeV pp collisions at ATLAS. *JHEP* **07**, 154 (2014). [https://doi.org/10.1007/JHEP07\(2014\)154](https://doi.org/10.1007/JHEP07(2014)154). arXiv:1404.7035
38. ATLAS Collaboration, The ATLAS experiment at the CERN large hadron collider. *JINST* **3**, S08003 (2008). <https://doi.org/10.1088/1748-0221/3/08/S08003>
39. ATLAS Collaboration, The ATLAS collaboration software and firmware. Technical report, CERN (2021). <https://cds.cern.ch/record/2767187>
40. ATLAS Collaboration, Muon reconstruction performance of the ATLAS detector in proton–proton collision data at $\sqrt{s} = 13$ TeV. *Eur. Phys. J. C* **76**, 292 (2016). <https://doi.org/10.1140/epjc/s10052-016-4120-y>. arXiv:1603.05598
41. M. Oreglia, A Study of the Reactions $\psi' \rightarrow \gamma\gamma\psi$. PhD thesis, Stanford University (1980). SLAC-R-236
42. Particle Data Group, P. Zyla et al., Review of particle physics. *PTEP* **2020**, 083C01 (2020). <https://doi.org/10.1093/ptep/ptaa104>
43. T. Sjöstrand et al., An introduction to PYTHIA 8.2. *Comput. Phys. Commun.* **191**, 159 (2015). <https://doi.org/10.1016/j.cpc.2015.01.024>. arXiv:1410.3012
44. ATLAS Collaboration, ATLAS Pythia 8 tunes to 7 TeV data. Technical report, CERN. (2014). <https://cds.cern.ch/record/1966419>
45. ATLAS Collaboration, The ATLAS simulation infrastructure. *Eur. Phys. J. C* **70**, 823 (2010). <https://doi.org/10.1140/epjc/s10052-010-1429-9>. arXiv:1005.4568
46. S. Agostinelli et al., Geant4—a simulation toolkit. *Nucl. Instrum. Methods A* **506**, 250 (2003). [https://doi.org/10.1016/S0168-9002\(03\)01368-8](https://doi.org/10.1016/S0168-9002(03)01368-8)
47. ATLAS Collaboration, Luminosity determination in pp collisions at $\sqrt{s} = 13$ TeV using the ATLAS detector at the LHC (2022). *Eur. Phys. J. C* **83**, 982 (2023). <https://doi.org/10.1140/epjc/s10052-023-11747-w>. arXiv:2212.09379
48. G. Avoni et al., The new LUCID-2 detector for luminosity measurement and monitoring in ATLAS. *JINST* **13**, P07017 (2018). <https://doi.org/10.1088/1748-0221/13/07/P07017>
49. CDF Collaboration, Measurement of J/ψ and $\psi(2S)$ polarization in $p\bar{p}$ collisions at $\sqrt{s} = 1.8$ TeV. *Phys. Rev. Lett.* **85**, 2886 (2000). <https://doi.org/10.1103/PhysRevLett.85.2886>
50. Y.-Q. Ma, T. Stebel, R. Venugopalan, J/ψ polarization in the CGC+NRQCD approach. *JHEP* **12**, 057 (2018). [https://doi.org/10.1007/JHEP12\(2018\)057](https://doi.org/10.1007/JHEP12(2018)057). arXiv:1809.03573
51. Y. Feng, B. Gong, C.-H. Chang, J.-X. Wang, Remaining parts of the long-standing J/ψ polarization puzzle. *Phys. Rev. D* **99**, 014044 (2019). <https://doi.org/10.1103/PhysRevD.99.014044>. arXiv:1810.08989
52. P. Faccioli, C. Lourenço, On the polarization of the non-prompt contribution to inclusive J/ψ production in pp collisions. *JHEP* **10**, 005 (2022). [https://doi.org/10.1007/JHEP10\(2022\)010](https://doi.org/10.1007/JHEP10(2022)010). arXiv:2206.14686
53. M. Butenschön, B.A. Kniehl, Reconciling J/ψ production at HERA, RHIC, Tevatron, and LHC with nonrelativistic QCD factorization at next-to-leading order. *Phys. Rev. Lett.* **106**, 022003 (2011). <https://doi.org/10.1103/PhysRevLett.106.022003>
54. M. Butenschoen, B.A. Kniehl, World data of J/ψ production consolidate nonrelativistic QCD factorization at next-to-leading order. *Phys. Rev. D* **84**, 051501 (2011). <https://doi.org/10.1103/PhysRevD.84.051501>
55. M. Butenschoen, B.A. Kniehl, Global analysis of $\psi(2S)$ inclusive hadroproduction at next-to-leading order in nonrelativistic-QCD factorization. *Phys. Rev. D* **107**, 034003 (2023). <https://doi.org/10.1103/PhysRevD.107.034003>. arXiv:2207.09346
56. S.P. Baranov, A.V. Lipatov, N.P. Zotov, Prompt charmonia production and polarization at LHC in the NRQCD with k_T -factorization. Part I: $\psi(2S)$ meson. *Eur. Phys. J. C* **75**, 455 (2015). <https://doi.org/10.1140/epjc/s10052-015-3689-x>. arXiv:1508.05480
57. S.P. Baranov, A.V. Lipatov, Prompt charmonia production and polarization at the LHC in the NRQCD with k_T -factorization. III. J/ψ meson. *Phys. Rev. D* **96**, 034019 (2017). <https://doi.org/10.1103/PhysRevD.96.034019>

58. A.V. Lipatov, M.A. Malyshev, S.P. Baranov, Particle event generator: a simple-in-use system PEGASUS version 1.0. *Eur. Phys. J. C* **80**, 330 (2020). <https://doi.org/10.1140/epjc/s10052-020-7898-6>. arXiv:1912.04204
59. S.P. Baranov, A.V. Lipatov, Are there any challenges in the charmonia production and polarization at the LHC? *Phys. Rev. D* **100**, 114021 (2019). <https://doi.org/10.1103/PhysRevD.100.114021>
60. H. Jung, Un-integrated PDFs in CCFM, in *12th International Workshop on Deep Inelastic Scattering (DIS 2004)*, p. 15 (2004). arXiv:hep-ph/0411287
61. V. Cheung, R. Vogt, Production and polarization of direct J/ψ to $\mathcal{O}(\alpha_s^3)$ in the improved color evaporation model in collinear factorization. *Phys. Rev. D* **104**, 094026 (2021). <https://doi.org/10.1103/PhysRevD.104.094026>
62. LHCb Collaboration, Measurement of J/ψ production in pp collisions at $\sqrt{s} = 7$ TeV. *Eur. Phys. J. C* **71**, 1645 (2011). <https://doi.org/10.1140/epjc/s10052-011-1645-y>. arXiv:1103.0423
63. M. Cacciari, FONLL heavy quark production. <http://www.lpthe.jussieu.fr/~cacciari/fonll/fonllform.html>. Accessed 03 Sept 2019
64. P. Bolzoni, B.A. Kniehl, G. Kramer, Inclusive J/ψ and $\psi(2S)$ production from b -hadron decay in $p\bar{p}$ and pp collisions. *Phys. Rev. D* **88**, 074035 (2013). <https://doi.org/10.1103/PhysRevD.88.074035>
65. B.A. Kniehl, G. Kramer, I. Schienbein, H. Spiesberger, Cross sections of inclusive $\psi(2S)$ and $X(3872)$ production from b -hadron decays in pp collisions and comparison with ATLAS, CMS, and LHCb data. *Phys. Rev. D* **103**, 094002 (2021). <https://doi.org/10.1103/PhysRevD.103.094002>
66. S.P. Baranov, A.V. Lipatov, M.A. Malyshev, Associated non-prompt $J/\psi + \mu$ and $J/\psi + J/\psi$ production at LHC as a test for TMD gluon density. *Eur. Phys. J. C* **78**, 820 (2018). <https://doi.org/10.1140/epjc/s10052-018-6297-8>. arXiv:1808.06233
67. ATLAS Collaboration, ATLAS computing acknowledgements. ATL-SOFT-PUB-2023-001 (2023). <https://cds.cern.ch/record/2869272>

ATLAS Collaboration*

G. Aad¹⁰², B. Abbott¹²⁰, K. Abeling⁵⁵, N. J. Abicht⁴⁹, S. H. Abidi²⁹, A. Aboulhorma^{35e}, H. Abramowicz¹⁵¹, H. Abreu¹⁵⁰, Y. Abulaiti¹¹⁷, B. S. Acharya^{69a,69b,m}, C. Adam Bourdarios⁴, L. Adamczyk^{86a}, S. V. Addepalli²⁶, M. J. Addison¹⁰¹, J. Adelman¹¹⁵, A. Adiguzel^{21c}, T. Adye¹³⁴, A. A. Affolder¹³⁶, Y. Afik³⁶, M. N. Agaras¹³, J. Agarwala^{73a,73b}, A. Aggarwal¹⁰⁰, C. Agheorghiesei^{27c}, A. Ahmad³⁶, F. Ahmadov^{38,y}, W. S. Ahmed¹⁰⁴, S. Ahuja⁹⁵, X. Ai^{62a}, G. Aielli^{76a,76b}, A. Aikot¹⁶³, M. Ait Tamlihat^{35e}, B. Aitbenkhik^{35a}, I. Aizenberg¹⁶⁹, M. Akbiyik¹⁰⁰, T. P. A. Åkesson⁹⁸, A. V. Akimov³⁷, D. Akiyama¹⁶⁸, N. N. Akolkar²⁴, K. Al Khoury⁴¹, G. L. Alberghi^{23b}, J. Albert¹⁶⁵, P. Albicocco⁵³, G. L. Albouy⁶⁰, S. Alderweireldt⁵², M. Aleksa³⁶, I. N. Aleksandrov³⁸, C. Alexa^{27b}, T. Alexopoulos¹⁰, F. Alfonsi^{23b}, M. Algren⁵⁶, M. Alhroob¹²⁰, B. Ali¹³², H. M. J. Ali⁹¹, S. Ali¹⁴⁸, S. W. Alibocus⁹², M. Aliev¹⁴⁵, G. Alimonti^{71a}, W. Alkakh⁵⁵, C. Allaire⁶⁶, B. M. M. Allbrooke¹⁴⁶, J. F. Allen⁵², C. A. Allendes Flores^{137f}, P. P. Allport²⁰, A. Aloisio^{72a,72b}, F. Alonso⁹⁰, C. Alpigiani¹³⁸, M. Alvarez Estevez^{83b}, A. Alvarez Fernandez¹⁰⁰, M. Alves Cardoso⁵⁶, M. G. Alviggi^{72a,72b}, M. Aly¹⁰¹, Y. Amaral Coutinho^{83b}, A. Ambler¹⁰⁴, C. Amelung³⁶, M. Ameri¹⁰¹, C. G. Ames¹⁰⁹, D. Amidei¹⁰⁶, S. P. Amor Dos Santos^{130a}, K. R. Amos¹⁶³, V. Ananiev¹²⁵, C. Anastopoulos¹³⁹, T. Andeen¹¹, J. K. Anders³⁶, S. Y. Andreev^{47a,47b}, A. Andreazza^{71a,71b}, S. Angelidakis⁹, A. Angerami^{41,ab}, A. V. Anisenkov³⁷, A. Annovi^{74a}, C. Antel⁵⁶, M. T. Anthony¹³⁹, E. Antipov¹⁴⁵, M. Antonelli⁵³, F. Anulli^{75a}, M. Aoki⁸⁴, T. Aoki¹⁵³, J. A. Aparisi Pozo¹⁶³, M. A. Aparo¹⁴⁶, L. Aperio Bella⁴⁸, C. Appelt¹⁸, A. Apyan²⁶, N. Aranzabal³⁶, S. J. Arbiol Val⁸⁷, C. Arcangeletti⁵³, A. T. H. Arce⁵¹, E. Arena⁹², J.-F. Arguin¹⁰⁸, S. Argyropoulos⁵⁴, J.-H. Arling⁴⁸, O. Arnaez⁴, H. Arnold¹¹⁴, G. Artoni^{75a,75b}, H. Asada¹¹¹, K. Asai¹¹⁸, S. Asai¹⁵³, N. A. Asbah⁶¹, K. Assamagan²⁹, R. Astalos^{28a}, S. Atashi¹⁶⁰, R. J. Atkin^{33a}, M. Atkinson¹⁶², H. Atmani^{35f}, P. A. Atmasiddha¹⁰⁶, K. Augsten¹³², S. Auricchio^{72a,72b}, A. D. Aurioi²⁰, V. A. Austrup¹⁰¹, G. Avolio³⁶, K. Axiotis⁵⁶, G. Azuelos^{108,ag}, D. Babal^{28b}, H. Bachacou¹³⁵, K. Bachas^{152,p}, A. Bachi³⁴, F. Backman^{47a,47b}, A. Badea⁶¹, T. M. Baer¹⁰⁶, P. Bagnaia^{75a,75b}, M. Bahmani¹⁸, A. J. Bailey¹⁶³, V. R. Bailey¹⁶², J. T. Baines¹³⁴, L. Baines⁹⁴, O. K. Baker¹⁷², E. Bakos¹⁵, D. Bakshi Gupta⁸, V. Balakrishnan¹²⁰, R. Balasubramanian¹¹⁴, E. M. Baldin³⁷, P. Balek^{86a}, E. Ballabene^{23a,23b}, F. Balli¹³⁵, L. M. Baltés^{63a}, W. K. Balunas³², J. Balz¹⁰⁰, E. Banas⁸⁷, M. Bandieramonte¹²⁹, A. Bandyopadhyay²⁴, S. Bansal²⁴, L. Barak¹⁵¹, M. Barakat⁴⁸, E. L. Barberio¹⁰⁵, D. Barberis^{57a,57b}, M. Barbero¹⁰², M. Z. Barel¹¹⁴, K. N. Barends^{33a}, T. Barillari¹¹⁰, M.-S. Barisits³⁶, T. Barklow¹⁴³, P. Baron¹²², D. A. Baron Moreno¹⁰¹, A. Baroncelli^{62a}, G. Barone²⁹, A. J. Barr¹²⁶, J. D. Barr⁹⁶, L. Barranco Navarro^{47a,47b}, F. Barreiro⁹⁹, J. Barreiro Guimarães da Costa^{14a}, U. Barron¹⁵¹, M. G. Barros Teixeira^{130a}, S. Barsov³⁷, F. Bartels^{63a}, R. Bartoldus¹⁴³, A. E. Barton⁹¹, P. Bartos^{28a}, A. Basan¹⁰⁰, M. Baselga⁴⁹, A. Bassalat^{66,b}, M. J. Basso^{156a}, C. R. Basson¹⁰¹, R. L. Bates⁵⁹, S. Batlamous^{35e}, J. R. Batley³², B. Batool¹⁴¹, M. Battaglia¹³⁶, D. Battulga¹⁸, M. Bause^{75a,75b}, M. Bauer³⁶, P. Bauer²⁴, L. T. Bazzano Hurrell³⁰, J. B. Beacham⁵¹, T. Beau¹²⁷, J. Y. Beauchamp⁹⁰, P. H. Beauchemin¹⁵⁸, F. Becherer⁵⁴, P. Bechtel²⁴, H. P. Beck^{19,o}, K. Becker¹⁶⁷, A. J. Beddall⁸², V. A. Bednyakov³⁸, C. P. Bee¹⁴⁵, L. J. Beemster¹⁵, T. A. Beermann³⁶, M. Begalli^{83d}, M. Begel²⁹, A. Behera¹⁴⁵, J. K. Behr⁴⁸, J. F. Beirer⁵⁵, F. Beisiegel²⁴, M. Belfkir¹⁵⁹, G. Bella¹⁵¹

L. Bellagamba^{23b}, A. Bellerive³⁴, P. Bellos²⁰, K. Beloborodov³⁷, D. Benckekroun^{35a}, F. Bendecca^{35a}, Y. Benhammou¹⁵¹, M. Benoit²⁹, J. R. Bensinger²⁶, S. Bentvelsen¹¹⁴, L. Beresford⁴⁸, M. Beretta⁵³, E. Bergeas Kuutmann¹⁶¹, N. Berger⁴, B. Bergmann¹³², J. Beringer^{17a}, G. Bernardi⁵, C. Bernius¹⁴³, F. U. Bernlochner²⁴, F. Bernon^{36,102}, A. Berrocal Guardia¹³, T. Berry⁹⁵, P. Berta¹³³, A. Berthold⁵⁰, I. A. Bertram⁹¹, S. Bethke¹¹⁰, A. Betti^{75a,75b}, A. J. Bevan⁹⁴, N. K. Bhalla⁵⁴, M. Bhamjee^{33c}, S. Bhatta¹⁴⁵, D. S. Bhattacharya¹⁶⁶, P. Bhattarai¹⁴³, V. S. Bhopatkar¹²¹, R. Bi^{29,aj}, R. M. Bianchi¹²⁹, G. Bianco^{23a,23b}, O. Biebel¹⁰⁹, R. Bielski¹²³, M. Biglietti^{77a}, M. Bindi⁵⁵, A. Bingul^{21b}, C. Bini^{75a,75b}, A. Biondini⁹², C. J. Birch-sykes¹⁰¹, G. A. Bird^{20,134}, M. Birman¹⁶⁹, M. Biros¹³³, S. Biryukov¹⁴⁶, T. Bisanz⁴⁹, E. Bisceglie^{43a,43b}, J. P. Biswal¹³⁴, D. Biswas¹⁴¹, A. Bitadze¹⁰¹, K. Bjørke¹²⁵, I. Bloch⁴⁸, C. Blocker²⁶, A. Blue⁵⁹, U. Blumenschein⁹⁴, J. Blumenthal¹⁰⁰, G. J. Bobbink¹¹⁴, V. S. Bobrovnikov³⁷, M. Boehler⁵⁴, B. Boehm¹⁶⁶, D. Bogavac³⁶, A. G. Bogdanchikov³⁷, C. Bohm^{47a}, V. Boisvert⁹⁵, P. Bokan⁴⁸, T. Bold^{86a}, M. Bomben⁵, M. Bona⁹⁴, M. Boonekamp¹³⁵, C. D. Booth⁹⁵, A. G. Borbély⁵⁹, I. S. Bordulev³⁷, H. M. Borecka-Bielska¹⁰⁸, G. Borissov⁹¹, D. Bortoletto¹²⁶, D. Boscherini^{23b}, M. Bosman¹³, J. D. Bossio Sola³⁶, K. Bouaouda^{35a}, N. Bouchhar¹⁶³, J. Boudreau¹²⁹, E. V. Bouhova-Thacker⁹¹, D. Boumediene⁴⁰, R. Bouquet¹⁶⁵, A. Boveia¹¹⁹, J. Boyd³⁶, D. Boye²⁹, I. R. Boyko³⁸, J. Bracinek²⁰, N. Brahimi^{62d}, G. Brandt¹⁷¹, O. Brandt³², F. Braren⁴⁸, B. Brau¹⁰³, J. E. Brau¹²³, R. Brener¹⁶⁹, L. Brenner¹¹⁴, R. Brenner¹⁶¹, S. Bressler¹⁶⁹, D. Britton⁵⁹, D. Britzger¹¹⁰, I. Brock²⁴, G. Brooijmans⁴¹, W. K. Brooks^{137f}, E. Brost²⁹, L. M. Brown¹⁶⁵, L. E. Bruce⁶¹, T. L. Bruckler¹²⁶, P. A. Bruckman de Renstrom⁸⁷, B. Brüers⁴⁸, A. Bruni^{23b}, G. Bruni^{23b}, M. Bruschi^{23b}, N. Brusino^{75a,75b}, T. Buanes¹⁶, Q. Buat¹³⁸, D. Buchin¹¹⁰, A. G. Buckley⁵⁹, O. Bulekov³⁷, B. A. Bullard¹⁴³, S. Burdin⁹², C. D. Burgard⁴⁹, A. M. Burger⁴⁰, B. Burghgrave⁸, O. Burlayenko⁵⁴, J. T. P. Burr³², C. D. Burton¹¹, J. C. Burzynski¹⁴², E. L. Busch⁴¹, V. Büscher¹⁰⁰, P. J. Bussey⁵⁹, J. M. Butler²⁵, C. M. Buttar⁵⁹, J. M. Butterworth⁹⁶, W. Buttinger¹³⁴, C. J. Buxo Vazquez¹⁰⁷, A. R. Buzykaev³⁷, S. Cabrera Urbán¹⁶³, L. Cadamuro⁶⁶, D. Caforio⁵⁸, H. Cai¹²⁹, Y. Cai^{14a,14e}, Y. Cai^{14c}, V. M. M. Cairo³⁶, O. Cakir^{3a}, N. Calace³⁶, P. Calafiura^{17a}, G. Calderini¹²⁷, P. Calfayan⁶⁸, G. Callea⁵⁹, L. P. Caloba^{83b}, D. Calvet⁴⁰, S. Calvet⁴⁰, T. P. Calvet¹⁰², M. Calvetti^{74a,74b}, R. Camacho Toro¹²⁷, S. Camarda³⁶, D. Camarero Munoz²⁶, P. Camarri^{76a,76b}, M. T. Camerlingo^{72a,72b}, D. Cameron³⁶, C. Camincher¹⁶⁵, M. Campanelli⁹⁶, A. Camplani⁴², V. Canale^{72a,72b}, A. Canesse¹⁰⁴, J. Cantero¹⁶³, Y. Cao¹⁶², F. Capocasa²⁶, M. Capua^{43a,43b}, A. Carbone^{71a,71b}, R. Cardarelli^{76a}, J. C. J. Cardenas⁸, F. Cardillo¹⁶³, G. Carducci^{43a,43b}, T. Carli³⁶, G. Carlino^{72a}, J. I. Carlotto¹³, B. T. Carlson^{129,q}, E. M. Carlson^{156a,165}, L. Carminati^{71a,71b}, A. Carnelli¹³⁵, M. Carnesale^{75a,75b}, S. Caron¹¹³, E. Carquin^{137f}, S. Carra^{71a}, G. Carratta^{23a,23b}, F. Carrio Argos^{33g}, J. W. S. Carter¹⁵⁵, T. M. Carter⁵², M. P. Casado^{13,i}, M. Caspar⁴⁸, F. L. Castillo⁴, L. Castillo Garcia¹³, V. Castillo Gimenez¹⁶³, N. F. Castro^{130a,130e}, A. Catinaccio³⁶, J. R. Catmore¹²⁵, V. Cavaliere²⁹, N. Cavalli^{23a,23b}, V. Cavasinni^{74a,74b}, Y. C. Cekmecelioglu⁴⁸, E. Celebi^{21a}, F. Celli¹²⁶, M. S. Centonze^{70a,70b}, V. Cepaitis⁵⁶, K. Cerny¹²², A. S. Cerqueira^{83a}, A. Cerri¹⁴⁶, L. Cerrito^{76a,76b}, F. Cerutti^{17a}, B. Cervato¹⁴¹, A. Cervelli^{23b}, G. Cesarini⁵³, S. A. Cetin⁸², Z. Chadi^{35a}, D. Chakraborty¹¹⁵, J. Chan¹⁷⁰, W. Y. Chan¹⁵³, J. D. Chapman³², E. Chapon¹³⁵, B. Chargeishvili^{149b}, D. G. Charlton²⁰, T. P. Charman⁹⁴, M. Chatterjee¹⁹, C. Chauhan¹³³, S. Chekanov⁶, S. V. Chekulaev^{156a}, G. A. Chelkov^{38,a}, A. Chen¹⁰⁶, B. Chen¹⁵¹, B. Chen¹⁶⁵, H. Chen^{14c}, H. Chen²⁹, J. Chen^{62c}, J. Chen¹⁴², M. Chen¹²⁶, S. Chen¹⁵³, S. J. Chen^{14c}, X. Chen^{62c,135}, X. Chen^{14b,af}, Y. Chen^{62a}, C. L. Cheng¹⁷⁰, H. C. Cheng^{64a}, S. Cheong¹⁴³, A. Cheplakov³⁸, E. Cheremushkina⁴⁸, E. Cherepanova¹¹⁴, R. Cherkaoui El Moursli^{35e}, E. Cheu⁷, K. Cheung⁶⁵, L. Chevalier¹³⁵, V. Chiarella⁵³, G. Chiarelli^{74a}, N. Chiedde¹⁰², G. Chiodini^{70a}, A. S. Chisholm²⁰, A. Chitan^{27b}, M. Chitishvili¹⁶³, M. V. Chizhov³⁸, K. Choi¹¹, A. R. Chomont^{75a,75b}, Y. Chou¹⁰³, E. Y. S. Chow¹¹³, T. Chowdhury^{33g}, K. L. Chu¹⁶⁹, M. C. Chu^{64a}, X. Chu^{14a,14e}, J. Chudoba¹³¹, J. J. Chwastowski⁸⁷, D. Cieri¹¹⁰, K. M. Ciesla^{86a}, V. Cindro⁹³, A. Ciocio^{17a}, F. Ciroto^{72a,72b}, Z. H. Citron^{169,k}, M. Citterio^{71a}, D. A. Ciubotaru^{27b}, B. M. Ciungu¹⁵⁵, A. Clark⁵⁶, P. J. Clark⁵², C. Clarry¹⁵⁵, J. M. Clavijo Columbie⁴⁸, S. E. Clawson⁴⁸, C. Clement^{47a,47b}, J. Clercx⁴⁸, L. Clissa^{23a,23b}, Y. Coadou¹⁰², M. Cobal^{69a,69c}, A. Coccaro^{57b}, R. F. Coelho Barrue^{130a}, R. Coelho Lopes De Sa¹⁰³, S. Coelli^{71a}, H. Cohen¹⁵¹, A. E. C. Coimbra^{71a,71b}, B. Cole⁴¹, J. Collot⁶⁰, P. Conde Muñoz^{130a,130g}, M. P. Connell^{33c}, S. H. Connell^{33c}, I. A. Connelly⁵⁹, E. I. Conroy¹²⁶, F. Conventi^{72a,ah}, H. G. Cooke²⁰, A. M. Cooper-Sarkar¹²⁶, A. Cordeiro Oudot Choi¹²⁷, L. D. Corpe⁴⁰, M. Corradi^{75a,75b}, F. Corriveau^{104,w}, A. Cortes-Gonzalez¹⁸, M. J. Costa¹⁶³, F. Costanza⁴, D. Costanzo¹³⁹, B. M. Cote¹¹⁹, G. Cowan⁹⁵, K. Cranmer¹⁷⁰, D. Cremonini^{23a,23b}, S. Crépe-Renaudin⁶⁰, F. Crescioli¹²⁷

M. Cristinziani¹⁴¹, M. Cristoforetti^{78a,78b}, V. Croft¹¹⁴, J. E. Crosby¹²¹, G. Crosetti^{43a,43b}, A. Cueto⁹⁹,
 T. Cuhadar Donszelmann¹⁶⁰, H. Cui^{14a,14c}, Z. Cui⁷, W. R. Cunningham⁵⁹, F. Curcio^{43a,43b}, P. Czodrowski³⁶,
 M. M. Czurylo^{63b}, M. J. Da Cunha Sargedas De Sousa^{57a,57b}, J. V. Da Fonseca Pinto^{83b}, C. Da Via¹⁰¹,
 W. Dabrowski^{86a}, T. Dado⁴⁹, S. Dahbi^{33g}, T. Dai¹⁰⁶, D. Dal Santo¹⁹, C. Dallapiccola¹⁰³, M. Dam⁴²,
 G. D'amen²⁹, V. D'Amico¹⁰⁹, J. Damp¹⁰⁰, J. R. Dandoy¹²⁸, M. F. Daneri³⁰, M. Danninger¹⁴², V. Dao³⁶,
 G. Darbo^{57b}, S. Darmora⁶, S. J. Das^{29,aj}, S. D'Auria^{71a,71b}, C. David^{156b}, T. Davidek¹³³, B. Davis-Purcell³⁴,
 I. Dawson⁹⁴, H. A. Day-hall¹³², K. De⁸, R. De Asmundis^{72a}, N. De Biase⁴⁸, S. De Castro^{23a,23b},
 N. De Groot¹¹³, P. de Jong¹¹⁴, H. De la Torre¹¹⁵, A. De Maria^{14c}, A. De Salvo^{75a}, U. De Sanctis^{76a,76b},
 A. De Santo¹⁴⁶, J. B. De Vivie De Regie⁶⁰, D. V. Dedovich³⁸, J. Degens¹¹⁴, A. M. Deiana⁴⁴, F. Del Corso^{23a,23b},
 J. Del Peso⁹⁹, F. Del Rio^{63a}, F. Deliot¹³⁵, C. M. Delitzsch⁴⁹, M. Della Pietra^{72a,72b}, D. Della Volpe⁵⁶,
 A. Dell'Acqua³⁶, L. Dell'Asta^{71a,71b}, M. Delmastro⁴, P. A. Delsart⁶⁰, S. Demers¹⁷², M. Demichev³⁸,
 S. P. Denisov³⁷, L. D'Eramo⁴⁰, D. Derendarz⁸⁷, F. Derue¹²⁷, P. Dervan⁹², K. Desch²⁴, C. Deutsch²⁴,
 F. A. Di Bello^{57a,57b}, A. Di Ciaccio^{76a,76b}, L. Di Ciaccio⁴, A. Di Domenico^{75a,75b}, C. Di Donato^{72a,72b},
 A. Di Girolamo³⁶, G. Di Gregorio³⁶, A. Di Luca^{78a,78b}, B. Di Micco^{77a,77b}, R. Di Nardo^{77a,77b}, C. Diaconu¹⁰²,
 M. Diamantopoulou³⁴, F. A. Dias¹¹⁴, T. Dias Do Vale¹⁴², M. A. Diaz^{137a,137b}, F. G. Diaz Capriles²⁴,
 M. Didenko¹⁶³, E. B. Diehl¹⁰⁶, L. Diehl⁵⁴, S. Díez Cornell⁴⁸, C. Díez Pardos¹⁴¹, C. Dimitriadi^{24,161},
 A. Dimitrievska^{17a}, J. Dingfelder²⁴, I.-M. Dinu^{27b}, S. J. Dittmeier^{63b}, F. Dittus³⁶, F. Djama¹⁰²,
 T. Djobava^{149b}, J. I. Djuvsland¹⁶, C. Doglioni^{98,101}, A. Dohmalova^{28a}, J. Dolejsi¹³³, Z. Dolezal¹³³,
 K. M. Dona³⁹, M. Donadelli^{83c}, B. Dong¹⁰⁷, J. Donini⁴⁰, A. D'Onofrio^{77a,77b}, M. D'Onofrio⁹²,
 J. Dopke¹³⁴, A. Doria^{72a}, N. Dos Santos Fernandes^{130a}, P. Dougan¹⁰¹, M. T. Dova⁹⁰, A. T. Doyle⁵⁹,
 M. A. Draguet¹²⁶, E. Dreyer¹⁶⁹, I. Drivas-koulouris¹⁰, M. Drnevich¹¹⁷, A. S. Drobac¹⁵⁸, M. Drozdova⁵⁶,
 D. Du^{62a}, T. A. du Pree¹¹⁴, F. Dubinin³⁷, M. Dubovsky^{28a}, E. Duchovni¹⁶⁹, G. Duckeck¹⁰⁹, O. A. Ducu^{27b},
 D. Duda⁵², A. Dudarev³⁶, E. R. Duden²⁶, M. D'uffizi¹⁰¹, L. Duflot⁶⁶, M. Dührssen³⁶, C. Dülsen¹⁷¹,
 A. E. Dumitriu^{27b}, M. Dunford^{63a}, S. Dungs⁴⁹, K. Dunne^{47a,47b}, A. Duperrin¹⁰², H. Duran Yildiz^{3a},
 M. Dören⁵⁸, A. Durglishvili^{149b}, B. L. Dwyer¹¹⁵, G. I. Dyckes^{17a}, M. Dyndal^{86a}, B. S. Dziedzic⁸⁷,
 Z. O. Earnshaw¹⁴⁶, G. H. Eberwein¹²⁶, B. Eckerova^{28a}, S. Eggebrecht⁵⁵, E. Egidio Purcino De Souza¹²⁷,
 L. F. Ehrke⁵⁶, G. Eigen¹⁶, K. Einsweiler^{17a}, T. Ekelof¹⁶¹, P. A. Ekman⁹⁸, S. El Farkh^{35b}, Y. El Ghazali^{35b},
 H. El Jarrari^{35e,148}, A. El Moussaouy¹⁰⁸, V. Ellajosyula¹⁶¹, M. Ellert¹⁶¹, F. Ellinghaus¹⁷¹, N. Ellis³⁶,
 J. Elmsheuser²⁹, M. Elsing³⁶, D. Emeliyanov¹³⁴, Y. Enari¹⁵³, I. Ene^{17a}, S. Epari¹³, J. Erdmann⁴⁹,
 P. A. Erland⁸⁷, M. Errenst¹⁷¹, M. Escalier⁶⁶, C. Escobar¹⁶³, E. Etzion¹⁵¹, G. Evans^{130a}, H. Evans⁶⁸,
 L. S. Evans⁹⁵, M. O. Evans¹⁴⁶, A. Ezhilov³⁷, S. Ezzarqtouni^{35a}, F. Fabbri⁵⁹, L. Fabbri^{23a,23b}, G. Facini⁹⁶,
 V. Fadeyev¹³⁶, R. M. Fakhruddinov³⁷, S. Falciano^{75a}, L. F. Falda Ulhoa Coelho³⁶, P. J. Falke²⁴, J. Faltova¹³³,
 C. Fan¹⁶², Y. Fan^{14a}, Y. Fang^{14a,14c}, M. Fantì^{71a,71b}, M. Faraj^{69a,69b}, Z. Farazpay⁹⁷, A. Farbin⁸,
 A. Farilla^{77a}, T. Farooque¹⁰⁷, S. M. Farrington⁵², F. Fassi^{35e}, D. Fassouliotis⁹, M. Faucci Giannelli^{76a,76b},
 W. J. Fawcett³², L. Fayard⁶⁶, P. Federic¹³³, P. Federicova¹³¹, O. L. Fedin^{37,a}, G. Fedotov³⁷, M. Feickert¹⁷⁰,
 L. Feligioni¹⁰², D. E. Fellers¹²³, C. Feng^{62b}, M. Feng^{14b}, Z. Feng¹¹⁴, M. J. Fenton¹⁶⁰, A. B. Fenyuk³⁷,
 L. Ferencz⁴⁸, R. A. M. Ferguson⁹¹, S. I. Fernandez Luengo^{137f}, P. Fernandez Martinez¹³, M. J. V. Fernoux¹⁰²,
 J. Ferrando⁴⁸, A. Ferrari¹⁶¹, P. Ferrari^{113,114}, R. Ferrari^{73a}, D. Ferrere⁵⁶, C. Ferretti¹⁰⁶, F. Fiedler¹⁰⁰,
 P. Fiedler¹³², A. Filipčič⁹³, E. K. Filmer¹, F. Filthaut¹¹³, M. C. N. Fiolhais^{130a,130c,c}, L. Fiorini¹⁶³,
 W. C. Fisher¹⁰⁷, T. Fitschen¹⁰¹, P. M. Fitzhugh¹³⁵, I. Fleck¹⁴¹, P. Fleischmann¹⁰⁶, T. Flick¹⁷¹, M. Flores^{33d,ac},
 L. R. Flores Castillo^{64a}, L. Flores Sanz De Acedo³⁶, F. M. Follega^{78a,78b}, N. Fomin¹⁶, J. H. Foo¹⁵⁵,
 B. C. Forland⁶⁸, A. Formica¹³⁵, A. C. Forti¹⁰¹, E. Fortin³⁶, A. W. Fortman⁶¹, M. G. Foti^{17a}, L. Fountas^{9,j},
 D. Fournier⁶⁶, H. Fox⁹¹, P. Francavilla^{74a,74b}, S. Francescato⁶¹, S. Franchellucci⁵⁶, M. Franchini^{23a,23b},
 S. Franchino^{63a}, D. Francis³⁶, L. Franco¹¹³, V. Franco Lima³⁶, L. Franconi⁴⁸, M. Franklin⁶¹, G. Frattari²⁶,
 A. C. Freegard⁹⁴, W. S. Freund^{83b}, Y. Y. Frid¹⁵¹, J. Friend⁵⁹, N. Fritzsche⁵⁰, A. Froch⁵⁴, D. Froidevaux³⁶,
 J. A. Frost¹²⁶, Y. Fu^{62a}, S. Fuenzalida Garrido^{137f}, M. Fujimoto^{118,ad}, E. Fullana Torregrosa^{163,*},
 K. Y. Fung^{64a}, E. Furtado De Simas Filho^{83b}, M. Furukawa¹⁵³, J. Fuster¹⁶³, A. Gabrielli^{23a,23b}, A. Gabrielli¹⁵⁵,
 P. Gadow³⁶, G. Gagliardi^{57a,57b}, L. G. Gagnon^{17a}, E. J. Gallas¹²⁶, B. J. Gallop¹³⁴, K. K. Gan¹¹⁹,
 S. Ganguly¹⁵³, Y. Gao⁵², F. M. Garay Walls^{137a,137b}, B. Garcia²⁹, C. García¹⁶³, A. Garcia Alonso¹¹⁴,
 A. G. Garcia Caffaro¹⁷², J. E. García Navarro¹⁶³, M. Garcia-Sciveres^{17a}, G. L. Gardner¹²⁸, R. W. Gardner³⁹,
 N. Garelli¹⁵⁸, D. Garg⁸⁰, R. B. Garg^{143,n}, J. M. Gargan⁵², C. A. Garner¹⁵⁵, C. M. Garvey^{33a}, P. Gaspar^{83b},
 V. K. Gassmann¹⁵⁸, G. Gaudio^{73a}, V. Gautam¹³, P. Gauzzi^{75a,75b}, I. L. Gavrilenko³⁷, A. Gavriluk³⁷,
 C. Gay¹⁶⁴, G. Gaycken⁴⁸, E. N. Gazis¹⁰, A. A. Geanta^{27b}, C. M. Gee¹³⁶, C. Gemme^{57b}, M. H. Genest⁶⁰,





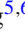
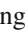
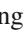
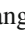

S. Gentile^{75a,75b}, A. D. Gentry¹¹², S. George⁹⁵, W. F. George²⁰, T. Geralis⁴⁶, P. Gessinger-Befurt³⁶, M. E. Geyik¹⁷¹, M. Ghani¹⁶⁷, M. Ghneimat¹⁴¹, K. Ghorbanian⁹⁴, A. Ghosal¹⁴¹, A. Ghosh¹⁶⁰, A. Ghosh⁷, B. Giacobbe^{23b}, S. Giagu^{75a,75b}, T. Giani¹¹⁴, P. Giannetti^{74a}, A. Giannini^{62a}, S. M. Gibson⁹⁵, M. Gignac¹³⁶, D. T. Gil^{86b}, A. K. Gilbert^{86a}, B. J. Gilbert⁴¹, D. Gillberg³⁴, G. Gilles¹¹⁴, N. E. K. Gillwald⁴⁸, L. Ginabat¹²⁷, D. M. Gingrich^{2,ag}, M. P. Giordani^{69a,69c}, P. F. Giraud¹³⁵, G. Giugliarelli^{69a,69c}, D. Giugni^{71a}, F. Giuli³⁶, I. Gkialas^{9j}, L. K. Gladilin³⁷, C. Glasman⁹⁹, G. R. Gledhill¹²³, G. Glemža⁴⁸, M. Glisic¹²³, I. Gnesi^{43b,f}, Y. Go^{29,aj}, M. Goblirsch-Kolb³⁶, B. Gocke⁴⁹, D. Godin¹⁰⁸, B. Gokturk^{21a}, S. Goldfarb¹⁰⁵, T. Golling⁵⁶, M. G. D. Gololo^{33g}, D. Golubkov³⁷, J. P. Gombas¹⁰⁷, A. Gomes^{130a,130b}, G. Gomes Da Silva¹⁴¹, A. J. Gomez Delegido¹⁶³, R. Gonçalo^{130a,130c}, G. Gonella¹²³, L. Gonella²⁰, A. Gongadze^{149c}, F. Gonnella²⁰, J. L. Gonski⁴¹, R. Y. González Andana⁵², S. González de la Hoz¹⁶³, S. Gonzalez Fernandez¹³, R. Gonzalez Lopez⁹², C. Gonzalez Renteria^{17a}, M. V. Gonzalez Rodrigues⁴⁸, R. Gonzalez Suarez¹⁶¹, S. Gonzalez-Sevilla⁵⁶, G. R. Gonzalvo Rodriguez¹⁶³, L. Goossens³⁶, B. Gorini³⁶, E. Gorini^{70a,70b}, A. Gorišek⁹³, T. C. Gosart¹²⁸, A. T. Goshaw⁵¹, M. I. Gostkin³⁸, S. Goswami¹²¹, C. A. Gottardo³⁶, S. A. Gotz¹⁰⁹, M. Gouighri^{35b}, V. Goumarre⁴⁸, A. G. Goussiou¹³⁸, N. Govender^{33c}, I. Grabowska-Bold^{86a}, K. Graham³⁴, E. Gramstad¹²⁵, S. Grancagnolo^{70a,70b}, M. Grandi¹⁴⁶, C. M. Grant^{1,135}, P. M. Gravila^{27f}, F. G. Gravili^{70a,70b}, H. M. Gray^{17a}, M. Greco^{70a,70b}, C. Grefe²⁴, I. M. Gregor⁴⁸, P. Grenier¹⁴³, S. G. Grewe¹¹⁰, C. Grieco¹³, A. A. Grillo¹³⁶, K. Grimm³¹, S. Grinstein^{13,s}, J.-F. Grivaz⁶⁶, E. Gross¹⁶⁹, J. Grosse-Knetter⁵⁵, C. Grud¹⁰⁶, J. C. Grundy¹²⁶, L. Guan¹⁰⁶, W. Guan²⁹, C. Gubbels¹⁶⁴, J. G. R. Guerrero Rojas¹⁶³, G. Guerrieri^{69a,69c}, F. Guescini¹¹⁰, R. Gugel¹⁰⁰, J. A. M. Guhit¹⁰⁶, A. Guida¹⁸, T. Guillemain⁴, E. Guillon^{134,167}, S. Guindon³⁶, F. Guo^{14a,14e}, J. Guo^{62c}, L. Guo⁴⁸, Y. Guo¹⁰⁶, R. Gupta⁴⁸, R. Gupta¹²⁹, S. Gurbuz²⁴, S. S. Gurdasani⁵⁴, G. Gustavino³⁶, M. Guth⁵⁶, P. Gutierrez¹²⁰, L. F. Gutierrez Zagazeta¹²⁸, M. Gutsche⁵⁰, C. Gutschow⁹⁶, C. Gwenlan¹²⁶, C. B. Gwilliam⁹², E. S. Haaland¹²⁵, A. Haas¹¹⁷, M. Habedank⁴⁸, C. Haber^{17a}, H. K. Hadavand⁸, A. Hadeef¹⁰⁰, S. Hadzic¹¹⁰, A. I. Hagan⁹¹, J. J. Hahn¹⁴¹, E. H. Haines⁹⁶, M. Haleem¹⁶⁶, J. Haley¹²¹, J. J. Hall¹³⁹, G. D. Hallewell¹⁰², L. Halser¹⁹, K. Hamano¹⁶⁵, M. Hamer²⁴, G. N. Hamity⁵², E. J. Hampshire⁹⁵, J. Han^{62b}, K. Han^{62a}, L. Han^{14c}, L. Han^{62a}, S. Han^{17a}, Y. F. Han¹⁵⁵, K. Hanagaki⁸⁴, M. Hance¹³⁶, D. A. Hangal^{41,ab}, H. Hanif¹⁴², M. D. Hank¹²⁸, R. Hankache¹⁰¹, J. B. Hansen⁴², J. D. Hansen⁴², P. H. Hansen⁴², K. Hara¹⁵⁷, D. Harada⁵⁶, T. Harenberg¹⁷¹, S. Harkusha³⁷, M. L. Harris¹⁰³, Y. T. Harris¹²⁶, J. Harrison¹³, N. M. Harrison¹¹⁹, P. F. Harrison¹⁶⁷, N. M. Hartman¹¹⁰, N. M. Hartmann¹⁰⁹, Y. Hasegawa¹⁴⁰, R. Hauser¹⁰⁷, C. M. Hawkes²⁰, R. J. Hawkings³⁶, Y. Hayashi¹⁵³, S. Hayashida¹¹¹, D. Hayden¹⁰⁷, C. Hayes¹⁰⁶, R. L. Hayes¹¹⁴, C. P. Hays¹²⁶, J. M. Hays⁹⁴, H. S. Hayward⁹², F. He^{62a}, M. He^{14a,14e}, Y. He¹⁵⁴, Y. He⁴⁸, N. B. Heatley⁹⁴, V. Hedberg⁹⁸, A. L. Heggelund¹²⁵, N. D. Hehir⁹⁴, C. Heidegger⁵⁴, K. K. Heidegger⁵⁴, W. D. Heidorn⁸¹, J. Heilman³⁴, S. Heim⁴⁸, T. Heim^{17a}, J. G. Heinlein¹²⁸, J. J. Heinrich¹²³, L. Heinrich^{110,ae}, J. Hejbal¹³¹, L. Helary⁴⁸, A. Held¹⁷⁰, S. Hellesund¹⁶, C. M. Helling¹⁶⁴, S. Hellman^{47a,47b}, R. C. W. Henderson⁹¹, L. Henkelmann³², A. M. Henriques Correia³⁶, H. Herde⁹⁸, Y. Hernández Jiménez¹⁴⁵, L. M. Herrmann²⁴, T. Herrmann⁵⁰, G. Herten⁵⁴, R. Hertenberger¹⁰⁹, L. Hervás³⁶, M. E. Hespings¹⁰⁰, N. P. Hessey^{156a}, H. Hibi⁸⁵, E. Hill¹⁵⁵, S. J. Hillier²⁰, J. R. Hinds¹⁰⁷, F. Hinterkeuser²⁴, M. Hirose¹²⁴, S. Hirose¹⁵⁷, D. Hirschbuehl¹⁷¹, T. G. Hitchings¹⁰¹, B. Hiti⁹³, J. Hobbs¹⁴⁵, R. Hobincu^{27e}, N. Hod¹⁶⁹, M. C. Hodgkinson¹³⁹, B. H. Hodkinson³², A. Hoecker³⁶, D. D. Hofer¹⁰⁶, J. Hofer⁴⁸, T. Holm²⁴, M. Holzbock¹¹⁰, L. B. A. H. Hommels³², B. P. Honan¹⁰¹, J. Hong^{62c}, T. M. Hong¹²⁹, B. H. Hooberman¹⁶², W. H. Hopkins⁶, Y. Horii¹¹¹, S. Hou¹⁴⁸, A. S. Howard⁹³, J. Howarth⁵⁹, J. Hoya⁶, M. Hrabovsky¹²², A. Hrynevich⁴⁸, T. Hryn'ova⁴, P. J. Hsu⁶⁵, S.-C. Hsu¹³⁸, Q. Hu^{62a}, Y. F. Hu^{14a,14e}, S. Huang^{64b}, X. Huang^{14c}, X. Huang^{14a,14e}, Y. Huang¹³⁹, Y. Huang^{14a}, Z. Huang¹⁰¹, Z. Hubacek¹³², M. Huebner²⁴, F. Huegging²⁴, T. B. Huffman¹²⁶, C. A. Hugli⁴⁸, M. Huhtinen³⁶, S. K. Huiberts¹⁶, R. Hulsken¹⁰⁴, N. Huseynov¹², J. Huston¹⁰⁷, J. Huth⁶¹, R. Hyneman¹⁴³, G. Iacobucci⁵⁶, G. Iakovidis²⁹, I. Ibragimov¹⁴¹, L. Iconomidou-Fayard⁶⁶, P. Iengo^{72a,72b}, R. Iguchi¹⁵³, T. Iizawa¹²⁶, Y. Ikegami⁸⁴, N. Ilic¹⁵⁵, H. Imam^{35a}, M. Ince Lezki⁵⁶, T. Ingebreten Carlson^{47a,47b}, G. Introzzi^{73a,73b}, M. Iodice^{77a}, V. Ippolito^{75a,75b}, R. K. Irwin⁹², M. Ishino¹⁵³, W. Islam¹⁷⁰, C. Issever^{18,48}, S. Istin^{21a,al}, H. Ito¹⁶⁸, J. M. Iturbe Ponce^{64a}, R. Iuppa^{78a,78b}, A. Ivina¹⁶⁹, J. M. Izen⁴⁵, V. Izzo^{72a}, P. Jacka^{131,132}, P. Jackson¹, R. M. Jacobs⁴⁸, B. P. Jaeger¹⁴², C. S. Jagfeld¹⁰⁹, G. Jain^{156a}, P. Jain⁵⁴, K. Jakobs⁵⁴, T. Jakoubek¹⁶⁹, J. Jamieson⁵⁹, K. W. Janas^{86a}, M. Javurkova¹⁰³, F. Jeanneau¹³⁵, L. Jeanty¹²³, J. Jejelava^{149a,z}, P. Jenni^{54,g}, C. E. Jessiman³⁴, S. Jézéquel⁴, C. Jia^{62b}, J. Jia¹⁴⁵, X. Jia⁶¹, X. Jia^{14a,14e}, Z. Jia^{14c}, S. Jiggins⁴⁸, J. Jimenez Pena¹³, S. Jin^{14c}, A. Jinaru^{27b}, O. Jinnouchi¹⁵⁴, P. Johansson¹³⁹, K. A. Johns⁷, J. W. Johnson¹³⁶, D. M. Jones³², E. Jones⁴⁸, P. Jones³², R. W. L. Jones⁹¹, T. J. Jones⁹², H. L. Joos^{36,55}

R. Joshi¹¹⁹, J. Jovicevic¹⁵, X. Ju^{17a}, J. J. Junggeburth¹⁰³, T. Junkermann^{63a}, A. Juste Rozas^{13,s}, M. K. Juzek⁸⁷, S. Kabana^{137e}, A. Kaczmarska⁸⁷, M. Kado¹¹⁰, H. Kagan¹¹⁹, M. Kagan¹⁴³, A. Kahn⁴¹, A. Kahn¹²⁸, C. Kahra¹⁰⁰, T. Kaji¹⁵³, E. Kajomovitz¹⁵⁰, N. Kakati¹⁶⁹, I. Kalaitzidou⁵⁴, C. W. Kalderon²⁹, A. Kamenshchikov¹⁵⁵, N. J. Kang¹³⁶, D. Kar^{33g}, K. Karava¹²⁶, M. J. Kareem^{156b}, E. Karentzos⁵⁴, I. Karkanas¹⁵², O. Karkout¹¹⁴, S. N. Karpov³⁸, Z. M. Karpova³⁸, V. Kartvelishvili⁹¹, A. N. Karyukhin³⁷, E. Kasimi¹⁵², J. Katzy⁴⁸, S. Kaur³⁴, K. Kawade¹⁴⁰, M. P. Kawale¹²⁰, C. Kawamoto⁸⁸, T. Kawamoto¹³⁵, E. F. Kay³⁶, F. I. Kaya¹⁵⁸, S. Kazakos¹⁰⁷, V. F. Kazanin³⁷, Y. Ke¹⁴⁵, J. M. Keaveney^{33a}, R. Keeler¹⁶⁵, G. V. Kehris⁶¹, J. S. Keller³⁴, A. S. Kelly⁹⁶, J. J. Kempster¹⁴⁶, K. E. Kennedy⁴¹, P. D. Kennedy¹⁰⁰, O. Kepka¹³¹, B. P. Kerridge¹⁶⁷, S. Kersten¹⁷¹, B. P. Kerševan⁹³, S. Keshri⁶⁶, L. Keszeghova^{28a}, S. Ketabchi Haghighat¹⁵⁵, R. A. Khan¹²⁹, M. Khandoga¹²⁷, A. Khanov¹²¹, A. G. Kharlamov³⁷, T. Kharlamova³⁷, E. E. Khoda¹³⁸, M. Kholodenko³⁷, T. J. Khoo¹⁸, G. Khoriauli¹⁶⁶, J. Khubua^{149b}, Y. A. R. Khwaira⁶⁶, A. Kilgallon¹²³, D. W. Kim^{47a,47b}, Y. K. Kim³⁹, N. Kimura⁹⁶, M. K. Kingston⁵⁵, A. Kirchhoff⁵⁵, C. Kirfel²⁴, F. Kirfel²⁴, J. Kirk¹³⁴, A. E. Kiryunin¹¹⁰, C. Kitsaki¹⁰, O. Kivernyk²⁴, M. Klassen^{63a}, C. Klein³⁴, L. Klein¹⁶⁶, M. H. Klein¹⁰⁶, M. Klein⁹², S. B. Klein⁵⁶, U. Klein⁹², P. Klimek³⁶, A. Klimentov²⁹, T. Klioutchnikova³⁶, P. Kluit¹¹⁴, S. Kluth¹¹⁰, E. Kneringer⁷⁹, T. M. Knight¹⁵⁵, A. Knue⁴⁹, R. Kobayashi⁸⁸, D. Kobylanski¹⁶⁹, S. F. Koch¹²⁶, M. Kocian¹⁴³, P. Kodyš¹³³, D. M. Koeck¹²³, P. T. Koenig²⁴, T. Koffas³⁴, O. Kolay⁵⁰, M. Kolb¹³⁵, I. Koletsou⁴, T. Komarek¹²², K. Köneke⁵⁴, A. X. Y. Kong¹, T. Kono¹¹⁸, N. Konstantinidis⁹⁶, P. Kontaxakis⁵⁶, B. Konya⁹⁸, S. Korn⁵⁵, S. Korn⁵⁵, I. Korolkov¹³, S. Koperny^{86a}, K. Korcyl⁸⁷, K. Kordas^{152,e}, G. Koren¹⁵¹, A. Korn⁹⁶, S. Korn⁵⁵, I. Korolkov¹³, N. Korotkova³⁷, B. Kortman¹¹⁴, O. Kortner¹¹⁰, S. Kortner¹¹⁰, W. H. Kostecka¹¹⁵, V. V. Kostyukhin¹⁴¹, A. Kotsokechagia¹³⁵, A. Kotwal⁵¹, A. Koulouris³⁶, A. Kourkoumeli-Charalampidi^{73a,73b}, C. Kourkoumelis⁹, E. Kourlitis^{110,ae}, O. Kovanda¹⁴⁶, R. Kowalewski¹⁶⁵, W. Kozanecki¹³⁵, A. S. Kozhin³⁷, V. A. Kramarenko³⁷, G. Kramberger⁹³, P. Kramer¹⁰⁰, M. W. Krasny¹²⁷, A. Krasznahorkay³⁶, J. W. Kraus¹⁷¹, J. A. Kremer⁴⁸, T. Kresse⁵⁰, J. Kretzschmar⁹², K. Kreul¹⁸, P. Krieger¹⁵⁵, S. Krishnamurthy¹⁰³, M. Krivos¹³³, K. Krizka²⁰, K. Kroeninger⁴⁹, H. Kroha¹¹⁰, J. Kroll¹³¹, J. Kroll¹²⁸, K. S. Krowpman¹⁰⁷, U. Kruchonak³⁸, H. Krüger²⁴, N. Krumnack⁸¹, M. C. Kruse⁵¹, J. A. Krzysiak⁸⁷, O. Kuchinskaia³⁷, S. Kuday^{3a}, S. Kuehn³⁶, R. Kuesters⁵⁴, T. Kuhl⁴⁸, V. Kukhtin³⁸, Y. Kulchitsky^{37,a}, S. Kuleshov^{137b,137d}, M. Kumar^{33g}, N. Kumari⁴⁸, A. Kupco¹³¹, T. Kupfer⁴⁹, A. Kupich³⁷, O. Kuprash⁵⁴, H. Kurashige⁸⁵, L. L. Kurchaninov^{156a}, O. Kurdysh⁶⁶, Y. A. Kurochkin³⁷, A. Kurova³⁷, M. Kuze¹⁵⁴, A. K. Kvam¹⁰³, J. Kvita¹²², T. Kwan¹⁰⁴, N. G. Kyriacou¹⁰⁶, L. A. O. Laatu¹⁰², C. Lacasta¹⁶³, F. Lacava^{75a,75b}, H. Lacker¹⁸, D. Lacour¹²⁷, N. N. Lad⁹⁶, E. Ladygin³⁸, B. Laforge¹²⁷, T. Lagouri^{137e}, F. Z. Lahbabi^{35a}, S. Lai⁵⁵, I. K. Lakomic^{86a}, N. Lalloue⁶⁰, J. E. Lambert¹⁶⁵, S. Lammers⁶⁸, W. Lampl⁷, C. Lampoudis^{152,e}, A. N. Lancaster¹¹⁵, E. Lançon²⁹, U. Landgraf⁵⁴, M. P. J. Landon⁹⁴, V. S. Lang⁵⁴, R. J. Langenberg¹⁰³, O. K. B. Langrekken¹²⁵, A. J. Lankford¹⁶⁰, F. Lanni³⁶, K. Lantzsch²⁴, A. Lanza^{73a}, A. Lapertosa^{57a,57b}, J. F. Laporte¹³⁵, T. Lari^{71a}, F. Lasagni Manghi^{23b}, M. Lassnig³⁶, V. Latonova¹³¹, A. Laudrain¹⁰⁰, A. Laurier¹⁵⁰, S. D. Lawlor¹³⁹, Z. Lawrence¹⁰¹, M. Lazzaroni^{71a,71b}, B. Le¹⁰¹, E. M. Le Boulicaut⁵¹, B. Leban⁹³, A. Lebedev⁸¹, M. LeBlanc¹⁰¹, F. Ledroit-Guillon⁶⁰, A. C. A. Lee⁹⁶, S. C. Lee¹⁴⁸, S. Lee^{47a,47b}, T. F. Lee⁹², L. L. Leeuw^{33c}, H. P. Lefebvre⁹⁵, M. Lefebvre¹⁶⁵, C. Leggett^{17a}, G. Lehmann Miotto³⁶, M. Leigh⁵⁶, W. A. Leight¹⁰³, W. Leinonen¹¹³, A. Leisos^{152,r}, M. A. L. Leite^{83c}, C. E. Leitgeb⁴⁸, R. Leitner¹³³, K. J. C. Leney⁴⁴, T. Lenz²⁴, S. Leone^{74a}, C. Leonidopoulos⁵², A. Leopold¹⁴⁴, C. Leroy¹⁰⁸, R. Les¹⁰⁷, C. G. Lester³², M. Levchenko³⁷, J. Levêque⁴, D. Levin¹⁰⁶, L. J. Levinson¹⁶⁹, M. P. Lewicki⁸⁷, D. J. Lewis⁴, A. Li⁵, B. Li^{62b}, C. Li^{62a}, C.-Q. Li^{62c}, H. Li^{62a}, H. Li^{62b}, H. Li^{14c}, H. Li^{14b}, H. Li^{62b}, J. Li^{62c}, K. Li¹³⁸, L. Li^{62c}, M. Li^{14a,14e}, Q. Y. Li^{62a}, S. Li^{14a,14e}, S. Li^{62c,62d,d}, T. Li⁵, X. Li¹⁰⁴, Z. Li¹²⁶, Z. Li¹⁰⁴, Z. Li⁹², Z. Li^{14a,14e}, S. Liang^{14a,14e}, Z. Liang^{14a}, M. Liberatore¹³⁵, B. Liberti^{76a}, K. Lie^{64c}, J. Lieber Marin^{83b}, H. Lien⁶⁸, K. Lin¹⁰⁷, R. E. Lindley⁷, J. H. Lindon², E. Lipeles¹²⁸, A. Lipniacka¹⁶, A. Lister¹⁶⁴, J. D. Little⁴, B. Liu^{14a}, B. X. Liu¹⁴², D. Liu^{62c,62d}, J. B. Liu^{62a}, J. K. K. Liu³², K. Liu^{62c,62d}, M. Liu^{62a}, M. Y. Liu^{62a}, P. Liu^{14a}, Q. Liu^{62c,62d,138}, X. Liu^{62a}, Y. Liu^{14d,14e}, Y. L. Liu^{62b}, Y. W. Liu^{62a}, J. Llorente Merino¹⁴², S. L. Lloyd⁹⁴, E. M. Lobodzinska⁴⁸, P. Loch⁷, T. Lohse¹⁸, K. Lohwasser¹³⁹, E. Loiacono⁴⁸, M. Lokajicek^{131,*}, J. D. Lomas²⁰, J. D. Long¹⁶², I. Longarini¹⁶⁰, L. Longo^{70a,70b}, R. Longo¹⁶², I. Lopez Paz⁶⁷, A. Lopez Solis⁴⁸, J. Lorenz¹⁰⁹, N. Lorenzo Martinez⁴, A. M. Lory¹⁰⁹, G. Lösckche Centeno¹⁴⁶, O. Loseva³⁷, X. Lou^{47a,47b}, X. Lou^{14a,14e}, A. Lounis⁶⁶, J. Love⁶, P. A. Love⁹¹, G. Lu^{14a,14e}, M. Lu⁸⁰, S. Lu¹²⁸, Y. J. Lu⁶⁵, H. J. Lubatti¹³⁸, C. Luci^{75a,75b}, F. L. Lucio Alves^{14c}, A. Lucotte⁶⁰, F. Luehring⁶⁸, I. Luise¹⁴⁵, O. Lukianchuk⁶⁶, O. Lundberg¹⁴⁴, B. Lund-Jensen¹⁴⁴, N. A. Luongo¹²³, M. S. Lutz¹⁵¹, A. B. Lux²⁵

R. Ospanov^{62a}, G. Otero y Garzon³⁰, H. Otono⁸⁹, P. S. Ott^{63a}, G. J. Ottino^{17a}, M. Ouchrif^{35d}, J. Ouellette²⁹, F. Ould-Saada¹²⁵, M. Owen⁵⁹, R. E. Owen¹³⁴, K. Y. Oyulmaz^{21a}, V. E. Ozcan^{21a}, F. Ozturk⁸⁷, N. Ozturk⁸, S. Ozturk⁸², H. A. Pacey¹²⁶, A. Pacheco Pages¹³, C. Padilla Aranda¹³, G. Padovano^{75a,75b}, S. Pagan Griso^{17a}, G. Palacino⁶⁸, A. Palazzo^{70a,70b}, S. Palestini³⁶, J. Pan¹⁷², T. Pan^{64a}, D. K. Panchal¹¹, C. E. Pandini¹¹⁴, J. G. Panduro Vazquez⁹⁵, H. D. Pandya¹, H. Pang^{14b}, P. Pani⁴⁸, G. Panizzo^{69a,69c}, L. Paolozzi⁵⁶, C. Papadatos¹⁰⁸, S. Parajuli⁴⁴, A. Paramonov⁶, C. Paraskevopoulos¹⁰, D. Paredes Hernandez^{64b}, K. R. Park⁴¹, T. H. Park¹⁵⁵, M. A. Parker³², F. Parodi^{57a,57b}, E. W. Parrish¹¹⁵, V. A. Parrish⁵², J. A. Parsons⁴¹, U. Parzefall⁵⁴, B. Pascual Dias¹⁰⁸, L. Pascual Dominguez¹⁵¹, E. Pasqualucci^{75a}, S. Passaggio^{57b}, F. Pastore⁹⁵, P. Pasuwan^{47a,47b}, P. Patel⁸⁷, U. M. Patel⁵¹, J. R. Pater¹⁰¹, T. Pauly³⁶, J. Parkes¹⁴³, M. Pedersen¹²⁵, R. Pedro^{130a}, S. V. Peleganchuk³⁷, O. Penc³⁶, E. A. Pender⁵², K. E. Pensi¹⁰⁹, M. Penzin³⁷, B. S. Peralva^{83d}, A. P. Pereira Peixoto⁶⁰, L. Pereira Sanchez^{47a,47b}, D. V. Perepelitsa^{29,aj}, E. Perez Codina^{156a}, M. Perganti¹⁰, L. Perini^{71a,71b,*}, H. Pernegger³⁶, O. Perrin⁴⁰, K. Peters⁴⁸, R. F. Y. Peters¹⁰¹, B. A. Petersen³⁶, T. C. Petersen⁴², E. Petit¹⁰², V. Petousis¹³², C. Petridou^{152,e}, A. Petrukhin¹⁴¹, M. Pettee^{17a}, N. E. Pettersson³⁶, A. Petukhov³⁷, K. Petukhova¹³³, R. Pezoa^{137f}, L. Pezzotti³⁶, G. Pezzullo¹⁷², T. M. Pham¹⁷⁰, T. Pham¹⁰⁵, P. W. Phillips¹³⁴, G. Piacquadio¹⁴⁵, E. Pianori^{17a}, F. Piazza¹²³, R. Piegai³⁰, D. Pietreanu^{27b}, A. D. Pilkington¹⁰¹, M. Pinamonti^{69a,69c}, J. L. Pinfold², B. C. Pinheiro Pereira^{130a}, A. E. Pinto Pinoargote^{100,135}, L. Pintucci^{69a,69c}, K. M. Piper¹⁴⁶, A. Pirttikoski⁵⁶, D. A. Pizzi³⁴, L. Pizzimento^{64b}, A. Pizzini¹¹⁴, M.-A. Pleier²⁹, V. Plesanovs⁵⁴, V. Pleskot¹³³, E. Plotnikova³⁸, G. Poddar⁴, R. Poettgen⁹⁸, L. Poggioli¹²⁷, I. Pokharel⁵⁵, S. Polacek¹³³, G. Polesello^{73a}, A. Poley^{142,156a}, R. Polifka¹³², A. Polini^{23b}, C. S. Pollard¹⁶⁷, Z. B. Pollock¹¹⁹, V. Polychronakos²⁹, E. Pompa Pacchi^{75a,75b}, D. Ponomarenko¹¹³, L. Pontecorvo³⁶, S. Popa^{27a}, G. A. Popeneciu^{27d}, A. Poreba³⁶, D. M. Portillo Quintero^{156a}, S. Pospisil¹³², M. A. Postill¹³⁹, P. Postolache^{27c}, K. Potamianos¹⁶⁷, P. A. Potepa^{86a}, I. N. Potrap³⁸, C. J. Potter³², H. Potti¹, T. Poulsen⁴⁸, J. Poveda¹⁶³, M. E. Pozo Astigarraga³⁶, A. Prades Ibanez¹⁶³, J. Pretel⁵⁴, D. Price¹⁰¹, M. Primavera^{70a}, M. A. Principe Martin⁹⁹, R. Privara¹²², T. Procter⁵⁹, M. L. Proffitt¹³⁸, N. Proklova¹²⁸, K. Prokofiev^{64c}, G. Proto¹¹⁰, S. Protopopescu²⁹, J. Proudfoot⁶, M. Przybycien^{86a}, W. W. Przygoda^{86b}, J. E. Puddefoot¹³⁹, D. Pudzha³⁷, D. Pyatizbyantseva³⁷, J. Qian¹⁰⁶, D. Qichen¹⁰¹, Y. Qin¹⁰¹, T. Qiu⁵², A. Quadt⁵⁵, M. Queitsch-Maitland¹⁰¹, G. Quetant⁵⁶, R. P. Quinn¹⁶⁴, G. Rabanal Bolanos⁶¹, D. Rafanoharana⁵⁴, F. Ragusa^{71a,71b}, J. L. Rainbolt³⁹, J. A. Raine⁵⁶, S. Rajagopalan²⁹, E. Ramakoti³⁷, I. A. Ramirez-Berend³⁴, K. Ran^{14e,48}, N. P. Rapheeha^{33g}, H. Rasheed^{27b}, V. Raskina¹²⁷, D. F. Rassloff^{63a}, S. Rave¹⁰⁰, B. Ravina⁵⁵, I. Ravinovich¹⁶⁹, M. Raymond³⁶, A. L. Read¹²⁵, N. P. Readioff¹³⁹, D. M. Rebuffi^{73a,73b}, G. Redlinger²⁹, A. S. Reed¹¹⁰, K. Reeves²⁶, J. A. Reidelsturz¹⁷¹, D. Reikher¹⁵¹, A. Rej⁴⁹, C. Rembser³⁶, A. Renardi⁴⁸, M. Renda^{27b}, M. B. Rendel¹¹⁰, F. Renner⁴⁸, A. G. Rennie¹⁶⁰, A. L. Rescia⁴⁸, S. Resconi^{71a}, M. Ressegotti^{57a,57b}, S. Rettie³⁶, J. G. Reyes Rivera¹⁰⁷, E. Reynolds^{17a}, O. L. Rezanova³⁷, P. Reznicek¹³³, N. Ribaric⁹¹, E. Ricci^{78a,78b}, R. Richter¹¹⁰, S. Richter^{47a,47b}, E. Richter-Was^{86b}, M. Ridel¹²⁷, S. Ridouani^{35d}, P. Rieck¹¹⁷, P. Riedler³⁶, E. M. Riefel^{47a,47b}, J. O. Rieger¹¹⁴, M. Rijssenbeek¹⁴⁵, A. Rimoldi^{73a,73b}, M. Rimoldi³⁶, L. Rinaldi^{23a,23b}, T. T. Rinn²⁹, M. P. Rinnagel¹⁰⁹, G. Ripellino¹⁶¹, I. Riu¹³, P. Rivadeneira⁴⁸, J. C. Rivera Vergara¹⁶⁵, F. Rizatdinova¹²¹, E. Rizvi⁹⁴, B. A. Roberts¹⁶⁷, B. R. Roberts^{17a}, S. H. Robertson^{104,w}, D. Robinson³², C. M. Robles Gajardo^{137f}, M. Robles Manzano¹⁰⁰, A. Robson⁵⁹, A. Rocchi^{76a,76b}, C. Roda^{74a,74b}, S. Rodriguez Bosca^{63a}, Y. Rodriguez Garcia^{22a}, A. Rodriguez Rodriguez⁵⁴, A. M. Rodríguez Vera^{156b}, S. Roe³⁶, J. T. Roemer¹⁶⁰, A. R. Roepe-Gier¹³⁶, J. Roggel¹⁷¹, O. Røhne¹²⁵, R. A. Rojas¹⁰³, C. P. A. Roland¹²⁷, J. Roloff²⁹, A. Romaniouk³⁷, E. Romano^{73a,73b}, M. Romano^{23b}, A. C. Romero Hernandez¹⁶², N. Rompotis⁹², L. Roos¹²⁷, S. Rosati^{75a}, B. J. Rosser³⁹, E. Rossi¹²⁶, E. Rossi^{72a,72b}, L. P. Rossi^{57b}, L. Rossini⁵⁴, R. Rosten¹¹⁹, M. Rotaru^{27b}, B. Rottler⁵⁴, C. Rougier^{102,aa}, D. Rousseau⁶⁶, D. Rousso³², A. Roy¹⁶², S. Roy-Garand¹⁵⁵, A. Rozanov¹⁰², Y. Rozen¹⁵⁰, X. Ruan^{33g}, A. Rubio Jimenez¹⁶³, A. J. Ruby⁹², V. H. Ruelas Rivera¹⁸, T. A. Ruggeri¹, A. Ruggiero¹²⁶, A. Ruiz-Martinez¹⁶³, A. Rummler³⁶, Z. Rurikova⁵⁴, N. A. Rusakovich³⁸, H. L. Russell¹⁶⁵, G. Russo^{75a,75b}, J. P. Rutherford⁷, S. Rutherford Colmenares³², K. Rybacki⁹¹, M. Rybar¹³³, E. B. Rye¹²⁵, A. Ryzhov⁴⁴, J. A. Sabater Iglesias⁵⁶, P. Sabatini¹⁶³, L. Sabetta^{75a,75b}, H. F.-W. Sadrozinski¹³⁶, F. Safai Tehrani^{75a}, B. Safarzadeh Samani¹³⁴, M. Safdari¹⁴³, S. Saha¹⁶⁵, M. Sahinsoy¹¹⁰, M. Saimpert¹³⁵, M. Saito¹⁵³, T. Saito¹⁵³, D. Salamani³⁶, A. Salnikov¹⁴³, J. Salt¹⁶³, A. Salvador Salas¹⁵¹, D. Salvatore^{43a,43b}, F. Salvatore¹⁴⁶, A. Salzburger³⁶, D. Sammel⁵⁴, D. Sampsonidis^{152,e}, D. Sampsonidou¹²³, J. Sánchez¹⁶³, A. Sanchez Pineda⁴, V. Sanchez Sebastian¹⁶³

H. Sandaker¹²⁵, C. O. Sander⁴⁸, J. A. Sandesara¹⁰³, M. Sandhoff¹⁷¹, C. Sandoval^{22b}, D. P. C. Sankey¹³⁴, T. Sano⁸⁸, A. Sansoni⁵³, L. Santi^{75a,75b}, C. Santoni⁴⁰, H. Santos^{130a,130b}, S. N. Santpur^{17a}, A. Santra¹⁶⁹, K. A. Saoucha^{116b}, J. G. Saraiva^{130a,130d}, J. Sardain⁷, O. Sasaki⁸⁴, K. Sato¹⁵⁷, C. Sauer^{63b}, F. Sauerburger⁵⁴, E. Sauvan⁴, P. Savard^{155.ag}, R. Sawada¹⁵³, C. Sawyer¹³⁴, L. Sawyer⁹⁷, I. Sayago Galvan¹⁶³, C. Sbarra^{23b}, A. Sbrizzi^{23a,23b}, T. Scanlon⁹⁶, J. Schaarschmidt¹³⁸, P. Schacht¹¹⁰, U. Schäfer¹⁰⁰, A. C. Schaffer^{44,66}, D. Schaile¹⁰⁹, R. D. Schamberger¹⁴⁵, C. Scharf¹⁸, M. M. Schefer¹⁹, V. A. Schegelsky³⁷, D. Scheirich¹³³, F. Schenck¹⁸, M. Schernau¹⁶⁰, C. Scheulen⁵⁵, C. Schiavi^{57a,57b}, E. J. Schioppa^{70a,70b}, M. Schioppa^{43a,43b}, B. Schlag^{143.n}, K. E. Schleicher⁵⁴, S. Schlenker³⁶, J. Schmeing¹⁷¹, M. A. Schmidt¹⁷¹, K. Schmieden¹⁰⁰, C. Schmitt¹⁰⁰, N. Schmitt¹⁰⁰, S. Schmitt⁴⁸, L. Schoeffel¹³⁵, A. Schoening^{63b}, P. G. Scholer⁵⁴, E. Schopf¹²⁶, M. Schott¹⁰⁰, J. Schovancova³⁶, S. Schramm⁵⁶, F. Schroeder¹⁷¹, T. Schroer⁵⁶, H.-C. Schultz-Coulon^{63a}, M. Schumacher⁵⁴, B. A. Schumm¹³⁶, Ph. Schune¹³⁵, A. J. Schuy¹³⁸, H. R. Schwartz¹³⁶, A. Schwartzman¹⁴³, T. A. Schwarz¹⁰⁶, Ph. Schwemling¹³⁵, R. Schwienhorst¹⁰⁷, A. Sciandra¹³⁶, G. Sciolla²⁶, F. Scuri^{74a}, C. D. Sebastiani⁹², K. Sedlaczek¹¹⁵, P. Seema¹⁸, S. C. Seidel¹¹², A. Seiden¹³⁶, B. D. Seidlitz⁴¹, C. Seitz⁴⁸, J. M. Seixas^{83b}, G. Sekhniaidze^{72a}, S. J. Sekula⁴⁴, L. Selem⁶⁰, N. Semprini-Cesari^{23a,23b}, D. Sengupta⁵⁶, V. Senthilkumar¹⁶³, L. Serin⁶⁶, L. Serkin^{69a,69b}, M. Sessa^{76a,76b}, H. Severini¹²⁰, F. Sforza^{57a,57b}, A. Sfyrta⁵⁶, E. Shabalina⁵⁵, R. Shaheen¹⁴⁴, J. D. Shahinian¹²⁸, D. Shaked Renous¹⁶⁹, L. Y. Shan^{14a}, M. Shapiro^{17a}, A. Sharma³⁶, A. S. Sharma¹⁶⁴, P. Sharma⁸⁰, S. Sharma⁴⁸, P. B. Shatalov³⁷, K. Shaw¹⁴⁶, S. M. Shaw¹⁰¹, A. Shcherbakova³⁷, Q. Shen^{5.62c}, P. Sherwood⁹⁶, L. Shi⁹⁶, X. Shi^{14a}, C. O. Shimmin¹⁷², J. D. Shinner⁹⁵, I. P. J. Shipsey¹²⁶, S. Shirabe^{56,h}, M. Shiyakova^{38,u}, J. Shlomi¹⁶⁹, M. J. Shochet³⁹, J. Shojaii¹⁰⁵, D. R. Shope¹²⁵, B. Shrestha¹²⁰, S. Shrestha^{119.ak}, E. M. Shrif^{33g}, M. J. Shroff¹⁶⁵, P. Sicho¹³¹, A. M. Sickles¹⁶², E. Sideras Haddad^{33g}, A. Sidoti^{23b}, F. Siegert⁵⁰, Dj. Sijacki¹⁵, R. Sikora^{86a}, F. Sili⁹⁰, J. M. Silva²⁰, M. V. Silva Oliveira²⁹, S. B. Silverstein^{47a}, S. Simion⁶⁶, R. Simoniello³⁶, E. L. Simpson⁵⁹, H. Simpson¹⁴⁶, L. R. Simpson¹⁰⁶, N. D. Simpson⁹⁸, S. Simsek⁸², S. Sindhu⁵⁵, P. Sinervo¹⁵⁵, S. Singh¹⁵⁵, S. Sinha⁴⁸, S. Sinha¹⁰¹, M. Sioli^{23a,23b}, I. Siral³⁶, E. Sitnikova⁴⁸, S. Yu. Sivoklov^{37,*}, J. Sjölin^{47a,47b}, A. Skaf⁵⁵, E. Skorda²⁰, P. Skubic¹²⁰, M. Slawinska⁸⁷, V. Smakhtin¹⁶⁹, B. H. Smart¹³⁴, J. Smiesko³⁶, S. Yu. Smirnov³⁷, Y. Smirnov³⁷, L. N. Smirnova^{37,a}, O. Smirnova⁹⁸, A. C. Smith⁴¹, E. A. Smith³⁹, H. A. Smith¹²⁶, J. L. Smith⁹², R. Smith¹⁴³, M. Smizanska⁹¹, K. Smolek¹³², A. A. Snesarev³⁷, S. R. Snider¹⁵⁵, H. L. Snoek¹¹⁴, S. Snyder²⁹, R. Sobie^{165.w}, A. Soffer¹⁵¹, C. A. Solans Sanchez³⁶, E. Yu. Soldatov³⁷, U. Soldevila¹⁶³, A. A. Solodkov³⁷, S. Solomon²⁶, A. Soloshenko³⁸, K. Solovieva⁵⁴, O. V. Solovyanov⁴⁰, V. Solovyev³⁷, P. Sommer³⁶, A. Sonay¹³, W. Y. Song^{156b}, J. M. Sonneveld¹¹⁴, A. Sopczak¹³², A. L. Sopio⁹⁶, F. Sopkova^{28b}, I. R. Sotarriva Alvarez¹⁵⁴, V. Sothilingam^{63a}, S. Sottocornola⁶⁸, R. Soualah^{116b}, Z. Soumami^{35e}, D. South⁴⁸, N. Soybelman¹⁶⁹, S. Spagnolo^{70a,70b}, M. Spalla¹¹⁰, D. Sperlich⁵⁴, G. Spigo³⁶, S. Spinali⁹¹, D. P. Spiteri⁵⁹, M. Spousta¹³³, E. J. Staats³⁴, A. Stabile^{71a,71b}, R. Stamen^{63a}, A. Stampekis²⁰, M. Standke²⁴, E. Stanecka⁸⁷, M. V. Stange⁵⁰, B. Stanislaus^{17a}, M. M. Stanitzki⁴⁸, B. Stapf⁴⁸, E. A. Starchenko³⁷, G. H. Stark¹³⁶, J. Stark^{102.aa}, D. M. Starke^{156b}, P. Staroba¹³¹, P. Starovoitov^{63a}, S. Stärz¹⁰⁴, R. Staszewski⁸⁷, G. Stavropoulos⁴⁶, J. Steentoft¹⁶¹, P. Steinberg²⁹, B. Stelzer^{142,156a}, H. J. Stelzer¹²⁹, O. Stelzer-Chilton^{156a}, H. Stenzel⁵⁸, T. J. Stevenson¹⁴⁶, G. A. Stewart³⁶, J. R. Stewart¹²¹, M. C. Stockton³⁶, G. Stoicea^{27b}, M. Stolarski^{130a}, S. Stonjek¹¹⁰, A. Straessner⁵⁰, J. Strandberg¹⁴⁴, S. Strandberg^{47a,47b}, M. Stratmann¹⁷¹, M. Strauss¹²⁰, T. Strebler¹⁰², P. Strizenec^{28b}, R. Ströhmer¹⁶⁶, D. M. Strom¹²³, L. R. Strom⁴⁸, R. Stroynowski⁴⁴, A. Strubig^{47a,47b}, S. A. Stucci²⁹, B. Stugu¹⁶, J. Stupak¹²⁰, N. A. Styles⁴⁸, D. Su¹⁴³, S. Su^{62a}, W. Su^{62d}, X. Su^{62a,66}, K. Sugizaki¹⁵³, V. V. Sulin³⁷, M. J. Sullivan⁹², D. M. S. Sultan^{78a,78b}, L. Sultanaliyeva³⁷, S. Sultansoy^{3b}, T. Sumida⁸⁸, S. Sun¹⁰⁶, S. Sun¹⁷⁰, O. Sunneborn Gudnadottir¹⁶¹, N. Sur¹⁰², M. R. Sutton¹⁴⁶, H. Suzuki¹⁵⁷, M. Svatos¹³¹, M. Swiatkowski^{156a}, T. Swirski¹⁶⁶, I. Sykora^{28a}, M. Sykora¹³³, T. Sykora¹³³, D. Ta¹⁰⁰, K. Tackmann^{48.t}, A. Taffard¹⁶⁰, R. Tafirout^{156a}, J. S. Tafoya Vargas⁶⁶, E. P. Takeva⁵², Y. Takubo⁸⁴, M. Talby¹⁰², A. A. Talyshev³⁷, K. C. Tam^{64b}, N. M. Tamir¹⁵¹, A. Tanaka¹⁵³, J. Tanaka¹⁵³, R. Tanaka⁶⁶, M. Tanasini^{57a,57b}, Z. Tao¹⁶⁴, S. Tapia Araya^{137f}, S. Tapprogge¹⁰⁰, A. Tarek Abouelfadl Mohamed¹⁰⁷, S. Tarem¹⁵⁰, K. Tariq^{14a}, G. Tarna^{27b,102}, G. F. Tartarelli^{71a}, P. Tas¹³³, M. Tasevsky¹³¹, E. Tassi^{43a,43b}, A. C. Tate¹⁶², G. Tateno¹⁵³, Y. Tayalati^{35e,v}, G. N. Taylor¹⁰⁵, W. Taylor^{156b}, A. S. Tee¹⁷⁰, R. Teixeira De Lima¹⁴³, P. Teixeira-Dias⁹⁵, J. J. Teoh¹⁵⁵, K. Terashi¹⁵³, J. Terron⁹⁹, S. Terzo¹³, M. Testa⁵³, R. J. Teuscher^{155.w}, A. Thaler⁷⁹, O. Theiner⁵⁶, N. Themistokleous⁵², T. Theveneaux-Pelzer¹⁰², O. Thielmann¹⁷¹, D. W. Thomas⁹⁵, J. P. Thomas²⁰, E. A. Thompson^{17a}, P. D. Thompson²⁰, E. Thomson¹²⁸, Y. Tian⁵⁵, V. Tikhomirov^{37.a}, Yu. A. Tikhonov³⁷, S. Timoshenko³⁷, D. Timoshyn¹³³, E. X. L. Ting¹, P. Tipton¹⁷², S. H. Tlou^{33g}, A. Tnourji⁴⁰, K. Todome¹⁵⁴, S. Todorova-Nova¹³³, S. Todt⁵⁰, M. Togawa⁸⁴,

J. Tojo⁸⁹, S. Tokár^{28a}, K. Tokushuku⁸⁴, O. Toldaiev⁶⁸, R. Tombs³², M. Tomoto^{84,111}, L. Tompkins^{143,n}, K. W. Topolnicki^{86b}, E. Torrence¹²³, H. Torres^{102,aa}, E. Torró Pastor¹⁶³, M. Toscani³⁰, C. Toscirri³⁹, M. Tost¹¹, D. R. Tovey¹³⁹, A. Traeet¹⁶, I. S. Trandafir^{27b}, T. Trefzger¹⁶⁶, A. Tricoli²⁹, I. M. Trigger^{156a}, S. Trincaz-Duvoid¹²⁷, D. A. Trischuk²⁶, B. Trocme⁶⁰, C. Troncon^{71a}, L. Truong^{33c}, M. Trzebinski⁸⁷, A. Trzupek⁸⁷, F. Tsai¹⁴⁵, M. Tsai¹⁰⁶, A. Tsiamis^{152,e}, P. V. Tsiareshka³⁷, S. Tsigaridas^{156a}, A. Tsirigotis^{152,r}, V. Tsiskaridze¹⁵⁵, E. G. Tskhadadze^{149a}, M. Tsopoulou^{152,e}, Y. Tsujikawa⁸⁸, I. I. Tsukerman³⁷, V. Tsulaia^{17a}, S. Tsuno⁸⁴, O. Tsur¹⁵⁰, K. Tsurii¹¹⁸, D. Tsybychev¹⁴⁵, Y. Tu^{64b}, A. Tudorache^{27b}, V. Tudorache^{27b}, A. N. Tuna³⁶, S. Turchikhin^{57a,57b}, I. Turk Cakir^{3a}, R. Turra^{71a}, T. Turtuvshin^{38,x}, P. M. Tuts⁴¹, S. Tzamarias^{152,e}, P. Tzanis¹⁰, E. Tzovara¹⁰⁰, F. Ukegawa¹⁵⁷, P. A. Ulloa Poblete^{137b,137c}, E. N. Umaka²⁹, G. Unal³⁶, M. Unal¹¹, A. Undrus²⁹, G. Unel¹⁶⁰, J. Urban^{28b}, P. Urquijo¹⁰⁵, P. Urrejola^{137a}, G. Usai⁸, R. Ushioda¹⁵⁴, M. Usman¹⁰⁸, Z. Uysal^{21b}, V. Vacek¹³², B. Vachon¹⁰⁴, K. O. H. Vadla¹²⁵, T. Vafeiadis³⁶, A. Vaitkus⁹⁶, C. Valderanis¹⁰⁹, E. Valdes Santurio^{47a,47b}, M. Valente^{156a}, S. Valentinetti^{23a,23b}, A. Valero¹⁶³, E. Valiente Moreno¹⁶³, A. Vallier^{102,aa}, J. A. Valls Ferrer¹⁶³, D. R. Van Arneman¹¹⁴, T. R. Van Daalen¹³⁸, A. Van Der Graaf⁴⁹, P. Van Gemmeren⁶, M. Van Rijnbach^{36,125}, S. Van Stroud⁹⁶, I. Van Vulpen¹¹⁴, M. Vanadia^{76a,76b}, W. Vandelli³⁶, M. Vandenbroucke¹³⁵, E. R. Vandewall¹²¹, D. Vannicola¹⁵¹, L. Vannoli^{57a,57b}, R. Vari^{75a}, E. W. Varnes⁷, C. Varni^{17b}, T. Varol¹⁴⁸, D. Varouchas⁶⁶, L. Varriale¹⁶³, K. E. Varvell¹⁴⁷, M. E. Vasile^{27b}, L. Vaslin⁸⁴, G. A. Vasquez¹⁶⁵, A. Vasyukov³⁸, F. Vazeille⁴⁰, T. Vazquez Schroeder³⁶, J. Veatch³¹, V. Vecchio¹⁰¹, M. J. Veen¹⁰³, I. Veliscek¹²⁶, L. M. Veloce¹⁵⁵, F. Veloso^{130a,130c}, S. Veneziano^{75a}, A. Ventura^{70a,70b}, S. Ventura Gonzalez¹³⁵, A. Verbytskyi¹¹⁰, M. Verducci^{74a,74b}, C. Vergis²⁴, M. Verissimo De Araujo^{83b}, W. Verkerke¹¹⁴, J. C. Vermeulen¹¹⁴, C. Vernieri¹⁴³, M. Vessella¹⁰³, M. C. Vetterli^{142,ag}, A. Vgenopoulos^{152,e}, N. Viaux Maira^{137f}, T. Vickey¹³⁹, O. E. Vickey Boeriu¹³⁹, G. H. A. Viehhauser¹²⁶, L. Vignani^{63b}, M. Villa^{23a,23b}, M. Villaplana Perez¹⁶³, E. M. Villhauer⁵², E. Vilucchi⁵³, M. G. Vincter³⁴, G. S. Virdee²⁰, A. Vishwakarma⁵², A. Visibile¹¹⁴, C. Vittori³⁶, I. Vivarelli¹⁴⁶, E. Voevodina¹¹⁰, F. Vogel¹⁰⁹, J. C. Voigt⁵⁰, P. Vokac¹³², Yu. Volkotrub^{86a}, J. Von Ahnen⁴⁸, E. Von Toerne²⁴, B. Vormwald³⁶, V. Vorobel¹³³, K. Vorobev³⁷, M. Vos¹⁶³, K. Voss¹⁴¹, J. H. Vosseveld⁹², M. Vozak¹¹⁴, L. Vozdecky⁹⁴, N. Vranjes¹⁵, M. Vranjes Milosavljevic¹⁵, M. Vreeswijk¹¹⁴, R. Vuillermet³⁶, O. Vujanovic¹⁰⁰, I. Vukotic³⁹, S. Wada¹⁵⁷, C. Wagner¹⁰³, J. M. Wagner^{17a}, W. Wagner¹⁷¹, S. Wahdan¹⁷¹, H. Wahlberg⁹⁰, M. Wakida¹¹¹, J. Walder¹³⁴, R. Walker¹⁰⁹, W. Walkowiak¹⁴¹, A. Wall¹²⁸, T. Wamorkar⁶, A. Z. Wang¹³⁶, C. Wang¹⁰⁰, C. Wang^{62c}, H. Wang^{17a}, J. Wang^{64a}, R.-J. Wang¹⁰⁰, R. Wang⁶¹, R. Wang⁶, S. M. Wang¹⁴⁸, S. Wang^{62b}, T. Wang^{62a}, W. T. Wang⁸⁰, W. Wang^{14a}, X. Wang^{14c}, X. Wang¹⁶², X. Wang^{62c}, Y. Wang^{62d}, Y. Wang^{14c}, Z. Wang¹⁰⁶, Z. Wang^{51,62c,62d}, Z. Wang¹⁰⁶, A. Warburton¹⁰⁴, R. J. Ward²⁰, N. Warrack⁵⁹, A. T. Watson²⁰, H. Watson⁵⁹, M. F. Watson²⁰, E. Watton^{59,134}, G. Watts¹³⁸, B. M. Waugh⁹⁶, C. Weber²⁹, H. A. Weber¹⁸, M. S. Weber¹⁹, S. M. Weber^{63a}, C. Wei^{62a}, Y. Wei¹²⁶, A. R. Weidberg¹²⁶, E. J. Weik¹¹⁷, J. Weingarten⁴⁹, M. Weirich¹⁰⁰, C. Weiser⁵⁴, C. J. Wells⁴⁸, T. Wenaus²⁹, B. Wendland⁴⁹, T. Wengler³⁶, N. S. Wenke¹¹⁰, N. Wermes²⁴, M. Wessels^{63a}, A. M. Wharton⁹¹, A. S. White⁶¹, A. White⁸, M. J. White¹, D. Whiteson¹⁶⁰, L. Wickremasinghe¹²⁴, W. Wiedenmann¹⁷⁰, C. Wiel⁵⁰, M. Wielers¹³⁴, C. Wiglesworth⁴², D. J. Wilbern¹²⁰, H. G. Wilkens³⁶, D. M. Williams⁴¹, H. H. Williams¹²⁸, S. Williams³², S. Willocq¹⁰³, B. J. Wilson¹⁰¹, P. J. Windischhofer³⁹, F. I. Winkel³⁰, F. Winklmeier¹²³, B. T. Winter⁵⁴, J. K. Winter¹⁰¹, M. Wittgen¹⁴³, M. Wobisch⁹⁷, Z. Wolffs¹¹⁴, J. Wollrath¹⁶⁰, M. W. Wolter⁸⁷, H. Wolters^{130a,130c}, A. F. Wongel⁴⁸, E. L. Woodward⁴¹, S. D. Worm⁴⁸, B. K. Wosiek⁸⁷, K. W. Woźniak⁸⁷, S. Wozniowski⁵⁵, K. Wraight⁵⁹, C. Wu²⁰, J. Wu^{14a,14c}, M. Wu^{64a}, M. Wu¹¹³, S. L. Wu¹⁷⁰, X. Wu⁵⁶, Y. Wu^{62a}, Z. Wu¹³⁵, J. Wuerzinger^{110,ac}, T. R. Wyatt¹⁰¹, B. M. Wynne⁵², S. Xella⁴², L. Xia^{14c}, M. Xia^{14b}, J. Xiang^{64c}, M. Xie^{62a}, X. Xie^{62a}, S. Xin^{14a,14c}, A. Xiong¹²³, J. Xiong^{17a}, D. Xu^{14a}, H. Xu^{62a}, L. Xu^{62a}, R. Xu¹²⁸, T. Xu¹⁰⁶, Y. Xu^{14b}, Z. Xu⁵², Z. Xu^{14a}, Z. Xu^{14c}, B. Yabsley¹⁴⁷, S. Yacoob^{33a}, Y. Yamaguchi¹⁵⁴, E. Yamashita¹⁵³, H. Yamauchi¹⁵⁷, T. Yamazaki^{17a}, Y. Yamazaki⁸⁵, J. Yan^{62c}, S. Yan¹²⁶, Z. Yan²⁵, H. J. Yang^{62c,62d}, H. T. Yang^{62a}, S. Yang^{62a}, T. Yang^{64c}, X. Yang³⁶, X. Yang^{14a}, Y. Yang⁴⁴, Y. Yang^{62a}, Z. Yang^{62a}, W.-M. Yao^{17a}, Y. C. Yap⁴⁸, H. Ye^{14c}, H. Ye⁵⁵, J. Ye^{14a}, S. Ye²⁹, X. Ye^{62a}, Y. Yeh⁹⁶, I. Yeletsikh³⁸, B. K. Yeo^{17b}, M. R. Yexley⁹⁶, P. Yin⁴¹, K. Yorita¹⁶⁸, S. Younas^{27b}, C. J. S. Young³⁶, C. Young¹⁴³, C. Yu^{14a,14e,ai}, Y. Yu^{62a}, M. Yuan¹⁰⁶, R. Yuan^{62b}, L. Yue⁹⁶, M. Zaazoua^{62a}, B. Zabinski⁸⁷, E. Zaid⁵², T. Zakareishvili^{149b}, N. Zakharchuk³⁴, S. Zambito⁵⁶, J. A. Zamora Saa^{137b,137d}, J. Zang¹⁵³, D. Zanzi⁵⁴, O. Zaplatilek¹³², C. Zeitnitz¹⁷¹, H. Zeng^{14a}, J. C. Zeng¹⁶², D. T. Zenger Jr.²⁶, O. Zenin³⁷, T. Ženiš^{28a}, S. Zenz⁹⁴, S. Zerradi^{35a}, D. Zerwas⁶⁶, M. Zhai^{14a,14c}, B. Zhang^{14c}, D. F. Zhang¹³⁹, J. Zhang^{62b}, J. Zhang⁶, K. Zhang^{14a,14c}, L. Zhang^{14c}, P. Zhang^{14a,14c}, R. Zhang¹⁷⁰, S. Zhang¹⁰⁶

S. Zhang⁴⁴ , T. Zhang¹⁵³ , X. Zhang^{62c} , X. Zhang^{62b} , Y. Zhang^{5,62c} , Y. Zhang⁹⁶ , Y. Zhang^{14c} , Z. Zhang^{17a} , Z. Zhang⁶⁶ , H. Zhao¹³⁸ , P. Zhao⁵¹ , T. Zhao^{62b} , Y. Zhao¹³⁶ , Z. Zhao^{62a} , A. Zhemchugov³⁸ , J. Zheng^{14c} , K. Zheng¹⁶² , X. Zheng^{62a} , Z. Zheng¹⁴³ , D. Zhong¹⁶² , B. Zhou¹⁰⁶ , H. Zhou⁷ , N. Zhou^{62c} , Y. Zhou⁷ , C. G. Zhu^{62b} , J. Zhu¹⁰⁶ , Y. Zhu^{62c} , Y. Zhu^{62a} , X. Zhuang^{14a} , K. Zhukov³⁷ , V. Zhulanov³⁷ , N. I. Zimine³⁸ , J. Zinsser^{63b} , M. Ziolkowski¹⁴¹ , L. Živković¹⁵ , A. Zoccoli^{23a,23b} , K. Zoch⁶¹ , T. G. Zorbas¹³⁹ , O. Zormpa⁴⁶ , W. Zou⁴¹ , L. Zwalinski³⁶

- ¹ Department of Physics, University of Adelaide, Adelaide, Australia
- ² Department of Physics, University of Alberta, Edmonton, AB, Canada
- ³ (a) Department of Physics, Ankara University, Ankara, Türkiye; (b) Division of Physics, TOBB University of Economics and Technology, Ankara, Türkiye
- ⁴ LAPP, Université Savoie Mont Blanc, CNRS/IN2P3, Annecy, France
- ⁵ APC, Université Paris Cité, CNRS/IN2P3, Paris, France
- ⁶ High Energy Physics Division, Argonne National Laboratory, Argonne, IL, USA
- ⁷ Department of Physics, University of Arizona, Tucson, AZ, USA
- ⁸ Department of Physics, University of Texas at Arlington, Arlington, TX, USA
- ⁹ Physics Department, National and Kapodistrian University of Athens, Athens, Greece
- ¹⁰ Physics Department, National Technical University of Athens, Zografou, Greece
- ¹¹ Department of Physics, University of Texas at Austin, Austin, TX, USA
- ¹² Institute of Physics, Azerbaijan Academy of Sciences, Baku, Azerbaijan
- ¹³ Institut de Física d'Altes Energies (IFAE), Barcelona Institute of Science and Technology, Barcelona, Spain
- ¹⁴ (a) Institute of High Energy Physics, Chinese Academy of Sciences, Beijing, China; (b) Physics Department, Tsinghua University, Beijing, China; (c) Department of Physics, Nanjing University, Nanjing, China; (d) School of Science, Shenzhen Campus of Sun Yat-sen University, Shenzhen, China; (e) University of Chinese Academy of Science (UCAS), Beijing, China
- ¹⁵ Institute of Physics, University of Belgrade, Belgrade, Serbia
- ¹⁶ Department for Physics and Technology, University of Bergen, Bergen, Norway
- ¹⁷ (a) Physics Division, Lawrence Berkeley National Laboratory, Berkeley, CA, USA; (b) University of California, Berkeley, CA, USA
- ¹⁸ Institut für Physik, Humboldt Universität zu Berlin, Berlin, Germany
- ¹⁹ Albert Einstein Center for Fundamental Physics and Laboratory for High Energy Physics, University of Bern, Bern, Switzerland
- ²⁰ School of Physics and Astronomy, University of Birmingham, Birmingham, UK
- ²¹ (a) Department of Physics, Bogazici University, Istanbul, Türkiye; (b) Department of Physics Engineering, Gaziantep University, Gaziantep, Türkiye; (c) Department of Physics, Istanbul University, Istanbul, Türkiye
- ²² (a) Facultad de Ciencias y Centro de Investigaciones, Universidad Antonio Nariño, Bogotá, Colombia; (b) Departamento de Física, Universidad Nacional de Colombia, Bogotá, Colombia
- ²³ (a) Dipartimento di Fisica e Astronomia A. Righi, Università di Bologna, Bologna, Italy; (b) INFN Sezione di Bologna, Bologna, Italy
- ²⁴ Physikalisches Institut, Universität Bonn, Bonn, Germany
- ²⁵ Department of Physics, Boston University, Boston, MA, USA
- ²⁶ Department of Physics, Brandeis University, Waltham, MA, USA
- ²⁷ (a) Transilvania University of Brasov, Brasov, Romania; (b) Horia Hulubei National Institute of Physics and Nuclear Engineering, Bucharest, Romania; (c) Department of Physics, Alexandru Ioan Cuza University of Iasi, Iasi, Romania; (d) Physics Department, National Institute for Research and Development of Isotopic and Molecular Technologies, Cluj-Napoca, Romania; (e) University Politehnica Bucharest, Bucharest, Romania; (f) West University in Timisoara, Timisoara, Romania; (g) Faculty of Physics, University of Bucharest, Bucharest, Romania
- ²⁸ (a) Faculty of Mathematics, Physics and Informatics, Comenius University, Bratislava, Slovak Republic; (b) Department of Subnuclear Physics, Institute of Experimental Physics of the Slovak Academy of Sciences, Kosice, Slovak Republic
- ²⁹ Physics Department, Brookhaven National Laboratory, Upton, NY, USA
- ³⁰ Departamento de Física, y CONICET, Facultad de Ciencias Exactas y Naturales, Instituto de Física de Buenos Aires (IFIBA), Universidad de Buenos Aires, Buenos Aires, Argentina
- ³¹ California State University, Long Beach, CA, USA

- ³² Cavendish Laboratory, University of Cambridge, Cambridge, UK
- ³³ (a)Department of Physics, University of Cape Town, Cape Town, South Africa; (b)iThemba Labs, Western Cape, South Africa; (c)Department of Mechanical Engineering Science, University of Johannesburg, Johannesburg, South Africa; (d)National Institute of Physics, University of the Philippines Diliman, Quezon City, Philippines; (e)Department of Physics, University of South Africa, Pretoria, South Africa; (f)University of Zululand, KwaDlangezwa, Richards Bay, South Africa; (g)School of Physics, University of the Witwatersrand, Johannesburg, South Africa
- ³⁴ Department of Physics, Carleton University, Ottawa, ON, Canada
- ³⁵ (a)Faculté des Sciences Ain Chock, Réseau Universitaire de Physique des Hautes Energies-Université Hassan II, Casablanca, Morocco; (b)Faculté des Sciences, Université Ibn-Tofail, Kenitra, Morocco; (c)Faculté des Sciences Semlalia, Université Cadi Ayyad, LPHEA-Marrakech, Marrakech, Morocco; (d)LPMR, Faculté des Sciences, Université Mohamed Premier, Oujda, Morocco; (e)Faculté des sciences, Université Mohammed V, Rabat, Morocco; (f)Institute of Applied Physics, Mohammed VI Polytechnic University, Ben Guerir, Morocco
- ³⁶ CERN, Geneva, Switzerland
- ³⁷ Affiliated with an Institute Covered by a Cooperation Agreement with CERN, Geneva, Switzerland
- ³⁸ Affiliated with an International Laboratory Covered by a Cooperation Agreement with CERN, Geneva, Switzerland
- ³⁹ Enrico Fermi Institute, University of Chicago, Chicago, IL, USA
- ⁴⁰ LPC, Université Clermont Auvergne, CNRS/IN2P3, Clermont-Ferrand, France
- ⁴¹ Nevis Laboratory, Columbia University, Irvington, NY, USA
- ⁴² Niels Bohr Institute, University of Copenhagen, Copenhagen, Denmark
- ⁴³ (a)Dipartimento di Fisica, Università della Calabria, Rende, Italy; (b)INFN Gruppo Collegato di Cosenza, Laboratori Nazionali di Frascati, Frascati, Italy
- ⁴⁴ Physics Department, Southern Methodist University, Dallas, TX, USA
- ⁴⁵ Physics Department, University of Texas at Dallas, Richardson, TX, USA
- ⁴⁶ National Centre for Scientific Research “Demokritos”, Agia Paraskevi, Greece
- ⁴⁷ (a)Department of Physics, Stockholm University, Stockholm, Sweden; (b)Oskar Klein Centre, Stockholm, Sweden
- ⁴⁸ Deutsches Elektronen-Synchrotron DESY, Hamburg and Zeuthen, Germany
- ⁴⁹ Fakultät Physik, Technische Universität Dortmund, Dortmund, Germany
- ⁵⁰ Institut für Kern- und Teilchenphysik, Technische Universität Dresden, Dresden, Germany
- ⁵¹ Department of Physics, Duke University, Durham, NC, USA
- ⁵² SUPA-School of Physics and Astronomy, University of Edinburgh, Edinburgh, UK
- ⁵³ INFN e Laboratori Nazionali di Frascati, Frascati, Italy
- ⁵⁴ Physikalisches Institut, Albert-Ludwigs-Universität Freiburg, Freiburg, Germany
- ⁵⁵ II. Physikalisches Institut, Georg-August-Universität Göttingen, Göttingen, Germany
- ⁵⁶ Département de Physique Nucléaire et Corpusculaire, Université de Genève, Geneva, Switzerland
- ⁵⁷ (a)Dipartimento di Fisica, Università di Genova, Genoa, Italy; (b)INFN Sezione di Genova, Genoa, Italy
- ⁵⁸ II. Physikalisches Institut, Justus-Liebig-Universität Giessen, Giessen, Germany
- ⁵⁹ SUPA-School of Physics and Astronomy, University of Glasgow, Glasgow, UK
- ⁶⁰ LPSC, Université Grenoble Alpes, CNRS/IN2P3, Grenoble INP, Grenoble, France
- ⁶¹ Laboratory for Particle Physics and Cosmology, Harvard University, Cambridge, MA, USA
- ⁶² (a)Department of Modern Physics and State Key Laboratory of Particle Detection and Electronics, University of Science and Technology of China, Hefei, China; (b)Institute of Frontier and Interdisciplinary Science and Key Laboratory of Particle Physics and Particle Irradiation (MOE), Shandong University, Qingdao, China; (c)Key Laboratory for Particle Astrophysics and Cosmology (MOE), SKLPPC, School of Physics and Astronomy, Shanghai Jiao Tong University, Shanghai, China; (d)Tsung-Dao Lee Institute, Shanghai, China
- ⁶³ (a)Kirchhoff-Institut für Physik, Ruprecht-Karls-Universität Heidelberg, Heidelberg, Germany; (b)Physikalisches Institut, Ruprecht-Karls-Universität Heidelberg, Heidelberg, Germany
- ⁶⁴ (a)Department of Physics, Chinese University of Hong Kong, Shatin, N.T., Hong Kong, China; (b)Department of Physics, University of Hong Kong, Hong Kong, China; (c)Department of Physics and Institute for Advanced Study, Hong Kong University of Science and Technology, Clear Water Bay, Kowloon, Hong Kong, China
- ⁶⁵ Department of Physics, National Tsing Hua University, Hsinchu, Taiwan
- ⁶⁶ IJCLab, Université Paris-Saclay, CNRS/IN2P3, 91405 Orsay, France
- ⁶⁷ Centro Nacional de Microelectrónica (IMB-CNM-CSIC), Barcelona, Spain

- 68 Department of Physics, Indiana University, Bloomington, IN, USA
- 69 (a)INFN Gruppo Collegato di Udine, Sezione di Trieste, Udine, Italy; (b)ICTP, Trieste, Italy; (c)Dipartimento Politecnico di Ingegneria e Architettura, Università di Udine, Udine, Italy
- 70 (a)INFN Sezione di Lecce, Lecce, Italy; (b)Dipartimento di Matematica e Fisica, Università del Salento, Lecce, Italy
- 71 (a)INFN Sezione di Milano, Milan, Italy; (b)Dipartimento di Fisica, Università di Milano, Milan, Italy
- 72 (a)INFN Sezione di Napoli, Naples, Italy; (b)Dipartimento di Fisica, Università di Napoli, Naples, Italy
- 73 (a)INFN Sezione di Pavia, Pavia, Italy; (b)Dipartimento di Fisica, Università di Pavia, Pavia, Italy
- 74 (a)INFN Sezione di Pisa, Pisa, Italy; (b)Dipartimento di Fisica E. Fermi, Università di Pisa, Pisa, Italy
- 75 (a)INFN Sezione di Roma, Rome, Italy; (b)Dipartimento di Fisica, Sapienza Università di Roma, Rome, Italy
- 76 (a)INFN Sezione di Roma Tor Vergata, Rome, Italy; (b)Dipartimento di Fisica, Università di Roma Tor Vergata, Rome, Italy
- 77 (a)INFN Sezione di Roma Tre, Rome, Italy; (b)Dipartimento di Matematica e Fisica, Università Roma Tre, Rome, Italy
- 78 (a)INFN-TIFPA, Povo, Italy; (b)Università degli Studi di Trento, Trento, Italy
- 79 Department of Astro and Particle Physics, Universität Innsbruck, Innsbruck, Austria
- 80 University of Iowa, Iowa City, IA, USA
- 81 Department of Physics and Astronomy, Iowa State University, Ames, IA, USA
- 82 Istinye University, Sariyer, Istanbul, Türkiye
- 83 (a)Departamento de Engenharia Elétrica, Universidade Federal de Juiz de Fora (UFJF), Juiz de Fora, Brazil; (b)Universidade Federal do Rio De Janeiro COPPE/EE/IF, Rio de Janeiro, Brazil; (c)Instituto de Física, Universidade de São Paulo, São Paulo, Brazil; (d)Rio de Janeiro State University, Rio de Janeiro, Brazil
- 84 KEK, High Energy Accelerator Research Organization, Tsukuba, Japan
- 85 Graduate School of Science, Kobe University, Kobe, Japan
- 86 (a)Faculty of Physics and Applied Computer Science, AGH University of Krakow, Kraków, Poland; (b)Marian Smoluchowski Institute of Physics, Jagiellonian University, Kraków, Poland
- 87 Institute of Nuclear Physics Polish Academy of Sciences, Kraków, Poland
- 88 Faculty of Science, Kyoto University, Kyoto, Japan
- 89 Research Center for Advanced Particle Physics and Department of Physics, Kyushu University, Fukuoka, Japan
- 90 Instituto de Física La Plata, Universidad Nacional de La Plata and CONICET, La Plata, Argentina
- 91 Physics Department, Lancaster University, Lancaster, UK
- 92 Oliver Lodge Laboratory, University of Liverpool, Liverpool, UK
- 93 Department of Experimental Particle Physics, Jožef Stefan Institute and Department of Physics, University of Ljubljana, Ljubljana, Slovenia
- 94 School of Physics and Astronomy, Queen Mary University of London, London, UK
- 95 Department of Physics, Royal Holloway University of London, Egham, UK
- 96 Department of Physics and Astronomy, University College London, London, UK
- 97 Louisiana Tech University, Ruston, LA, USA
- 98 Fysiska institutionen, Lunds universitet, Lund, Sweden
- 99 Departamento de Física Teórica C-15 and CIAFF, Universidad Autónoma de Madrid, Madrid, Spain
- 100 Institut für Physik, Universität Mainz, Mainz, Germany
- 101 School of Physics and Astronomy, University of Manchester, Manchester, UK
- 102 CPPM, Aix-Marseille Université, CNRS/IN2P3, Marseille, France
- 103 Department of Physics, University of Massachusetts, Amherst, MA, USA
- 104 Department of Physics, McGill University, Montreal, QC, Canada
- 105 School of Physics, University of Melbourne, Melbourne, VIC, Australia
- 106 Department of Physics, University of Michigan, Ann Arbor, MI, USA
- 107 Department of Physics and Astronomy, Michigan State University, East Lansing, MI, USA
- 108 Group of Particle Physics, University of Montreal, Montreal, QC, Canada
- 109 Fakultät für Physik, Ludwig-Maximilians-Universität München, Munich, Germany
- 110 Max-Planck-Institut für Physik (Werner-Heisenberg-Institut), Munich, Germany
- 111 Graduate School of Science and Kobayashi-Maskawa Institute, Nagoya University, Nagoya, Japan
- 112 Department of Physics and Astronomy, University of New Mexico, Albuquerque, NM, USA
- 113 Institute for Mathematics, Astrophysics and Particle Physics, Radboud University/Nikhef, Nijmegen, The Netherlands
- 114 Nikhef National Institute for Subatomic Physics and University of Amsterdam, Amsterdam, The Netherlands

- 115 Department of Physics, Northern Illinois University, DeKalb, IL, USA
- 116 (a)New York University Abu Dhabi, Abu Dhabi, United Arab Emirates; (b)University of Sharjah, Sharjah, United Arab Emirates
- 117 Department of Physics, New York University, New York, NY, USA
- 118 Ochanomizu University, Otsuka, Bunkyo-ku, Tokyo, Japan
- 119 Ohio State University, Columbus, OH, USA
- 120 Homer L. Dodge Department of Physics and Astronomy, University of Oklahoma, Norman, OK, USA
- 121 Department of Physics, Oklahoma State University, Stillwater, OK, USA
- 122 Joint Laboratory of Optics, Palacký University, Olomouc, Czech Republic
- 123 Institute for Fundamental Science, University of Oregon, Eugene, OR, USA
- 124 Graduate School of Science, Osaka University, Osaka, Japan
- 125 Department of Physics, University of Oslo, Oslo, Norway
- 126 Department of Physics, Oxford University, Oxford, UK
- 127 LPNHE, Sorbonne Université, Université Paris Cité, CNRS/IN2P3, Paris, France
- 128 Department of Physics, University of Pennsylvania, Philadelphia, PA, USA
- 129 Department of Physics and Astronomy, University of Pittsburgh, Pittsburgh, PA, USA
- 130 (a)Laboratório de Instrumentação e Física Experimental de Partículas-LIP, Lisbon, Portugal; (b)Departamento de Física, Faculdade de Ciências, Universidade de Lisboa, Lisbon, Portugal; (c)Departamento de Física, Universidade de Coimbra, Coimbra, Portugal; (d)Centro de Física Nuclear da Universidade de Lisboa, Lisbon, Portugal; (e)Departamento de Física, Universidade do Minho, Braga, Portugal; (f)Departamento de Física Teórica y del Cosmos, Universidad de Granada, Granada, Spain; (g)Departamento de Física, Instituto Superior Técnico, Universidade de Lisboa, Lisbon, Portugal
- 131 Institute of Physics of the Czech Academy of Sciences, Prague, Czech Republic
- 132 Czech Technical University in Prague, Prague, Czech Republic
- 133 Faculty of Mathematics and Physics, Charles University, Prague, Czech Republic
- 134 Particle Physics Department, Rutherford Appleton Laboratory, Didcot, UK
- 135 IRFU, CEA, Université Paris-Saclay, Gif-sur-Yvette, France
- 136 Santa Cruz Institute for Particle Physics, University of California Santa Cruz, Santa Cruz, CA, USA
- 137 (a)Departamento de Física, Pontificia Universidad Católica de Chile, Santiago, Chile; (b)Millennium Institute for Subatomic Physics at High Energy Frontier (SAPHIR), Santiago, Chile; (c)Instituto de Investigación Multidisciplinario en Ciencia y Tecnología, y Departamento de Física, Universidad de La Serena, La Serena, Chile; (d)Department of Physics, Universidad Andres Bello, Santiago, Chile; (e)Instituto de Alta Investigación, Universidad de Tarapacá, Arica, Chile; (f)Departamento de Física, Universidad Técnica Federico Santa María, Valparaíso, Chile
- 138 Department of Physics, University of Washington, Seattle, WA, USA
- 139 Department of Physics and Astronomy, University of Sheffield, Sheffield, UK
- 140 Department of Physics, Shinshu University, Nagano, Japan
- 141 Department Physik, Universität Siegen, Siegen, Germany
- 142 Department of Physics, Simon Fraser University, Burnaby, BC, Canada
- 143 SLAC National Accelerator Laboratory, Stanford, CA, USA
- 144 Department of Physics, Royal Institute of Technology, Stockholm, Sweden
- 145 Departments of Physics and Astronomy, Stony Brook University, Stony Brook, NY, USA
- 146 Department of Physics and Astronomy, University of Sussex, Brighton, UK
- 147 School of Physics, University of Sydney, Sydney, Australia
- 148 Institute of Physics, Academia Sinica, Taipei, Taiwan
- 149 (a)E. Andronikashvili Institute of Physics, Iv. Javakhishvili Tbilisi State University, Tbilisi, Georgia; (b)High Energy Physics Institute, Tbilisi State University, Tbilisi, Georgia; (c)University of Georgia, Tbilisi, Georgia
- 150 Department of Physics, Technion, Israel Institute of Technology, Haifa, Israel
- 151 Raymond and Beverly Sackler School of Physics and Astronomy, Tel Aviv University, Tel Aviv, Israel
- 152 Department of Physics, Aristotle University of Thessaloniki, Thessaloniki, Greece
- 153 International Center for Elementary Particle Physics and Department of Physics, University of Tokyo, Tokyo, Japan
- 154 Department of Physics, Tokyo Institute of Technology, Tokyo, Japan
- 155 Department of Physics, University of Toronto, Toronto, ON, Canada
- 156 (a)TRIUMF, Vancouver, BC, Canada; (b)Department of Physics and Astronomy, York University, Toronto, ON, Canada

- 157 Division of Physics and Tomonaga Center for the History of the Universe, Faculty of Pure and Applied Sciences, University of Tsukuba, Tsukuba, Japan
- 158 Department of Physics and Astronomy, Tufts University, Medford, MA, USA
- 159 United Arab Emirates University, Al Ain, United Arab Emirates
- 160 Department of Physics and Astronomy, University of California Irvine, Irvine, CA, USA
- 161 Department of Physics and Astronomy, University of Uppsala, Uppsala, Sweden
- 162 Department of Physics, University of Illinois, Urbana, IL, USA
- 163 Instituto de Física Corpuscular (IFIC), Centro Mixto Universidad de Valencia-CSIC, Valencia, Spain
- 164 Department of Physics, University of British Columbia, Vancouver, BC, Canada
- 165 Department of Physics and Astronomy, University of Victoria, Victoria, BC, Canada
- 166 Fakultät für Physik und Astronomie, Julius-Maximilians-Universität Würzburg, Würzburg, Germany
- 167 Department of Physics, University of Warwick, Coventry, UK
- 168 Waseda University, Tokyo, Japan
- 169 Department of Particle Physics and Astrophysics, Weizmann Institute of Science, Rehovot, Israel
- 170 Department of Physics, University of Wisconsin, Madison, WI, USA
- 171 Fakultät für Mathematik und Naturwissenschaften, Fachgruppe Physik, Bergische Universität Wuppertal, Wuppertal, Germany
- 172 Department of Physics, Yale University, New Haven, CT, USA
- ^a Also Affiliated with an Institute Covered by a Cooperation Agreement with CERN, Geneva, Switzerland
- ^b Also at An-Najah National University, Nablus, Palestine
- ^c Also at Borough of Manhattan Community College, City University of New York, New York, NY, USA
- ^d Also at Center for High Energy Physics, Peking University, Beijing, China
- ^e Also at Center for Interdisciplinary Research and Innovation (CIRI-AUTH), Thessaloniki, Greece
- ^f Also at Centro Studi e Ricerche Enrico Fermi, Rome, Italy
- ^g Also at CERN, Geneva, Switzerland
- ^h Also at Département de Physique Nucléaire et Corpusculaire, Université de Genève, Geneva, Switzerland
- ⁱ Also at Departament de Física de la Universitat Autònoma de Barcelona, Barcelona, Spain
- ^j Also at Department of Financial and Management Engineering, University of the Aegean, Chios, Greece
- ^k Also at Department of Physics, Ben Gurion University of the Negev, Beersheba, Israel
- ^l Also at Department of Physics, California State University, Sacramento, USA
- ^m Also at Department of Physics, King's College London, London, UK
- ⁿ Also at Department of Physics, Stanford University, Stanford, CA, USA
- ^o Also at Department of Physics, University of Fribourg, Fribourg, Switzerland
- ^p Also at Department of Physics, University of Thessaly, Vólos, Greece
- ^q Also at Department of Physics, Westmont College, Santa Barbara, USA
- ^r Also at Hellenic Open University, Patras, Greece
- ^s Also at Institutio Catalana de Recerca i Estudis Avancats, ICREA, Barcelona, Spain
- ^t Also at Institut für Experimentalphysik, Universität Hamburg, Hamburg, Germany
- ^u Also at Institute for Nuclear Research and Nuclear Energy (INRNE) of the Bulgarian Academy of Sciences, Sofia, Bulgaria
- ^v Also at Institute of Applied Physics, Mohammed VI Polytechnic University, Ben Guerir, Morocco
- ^w Also at Institute of Particle Physics (IPP), Toronto, Canada
- ^x Also at Institute of Physics and Technology, Ulaanbaatar, Mongolia
- ^y Also at Institute of Physics, Azerbaijan Academy of Sciences, Baku, Azerbaijan
- ^z Also at Institute of Theoretical Physics, Ilia State University, Tbilisi, Georgia
- ^{aa} Also at L2IT, Université de Toulouse, CNRS/IN2P3, UPS, Toulouse, France
- ^{ab} Also at Lawrence Livermore National Laboratory, Livermore, USA
- ^{ac} Also at National Institute of Physics, University of the Philippines Diliman, Quezon City, Philippines
- ^{ad} Also at Ochanomizu University, Otsuka, Bunkyo-ku, Tokyo, Japan
- ^{ae} Also at Technical University of Munich, Munich, Germany
- ^{af} Also at The Collaborative Innovation Center of Quantum Matter (CICQM), Beijing, China
- ^{ag} Also at TRIUMF, Vancouver, BC, Canada

^{ah} Also at Università di Napoli Parthenope, Naples, Italy

^{ai} Also at University of Chinese Academy of Sciences (UCAS), Beijing, China

^{aj} Also at Department of Physics, University of Colorado Boulder, Colorado, USA

^{ak} Also at Washington College, Chestertown, MD, USA

^{al} Also at Physics Department, Yeditepe University, Istanbul, Türkiye

* Deceased